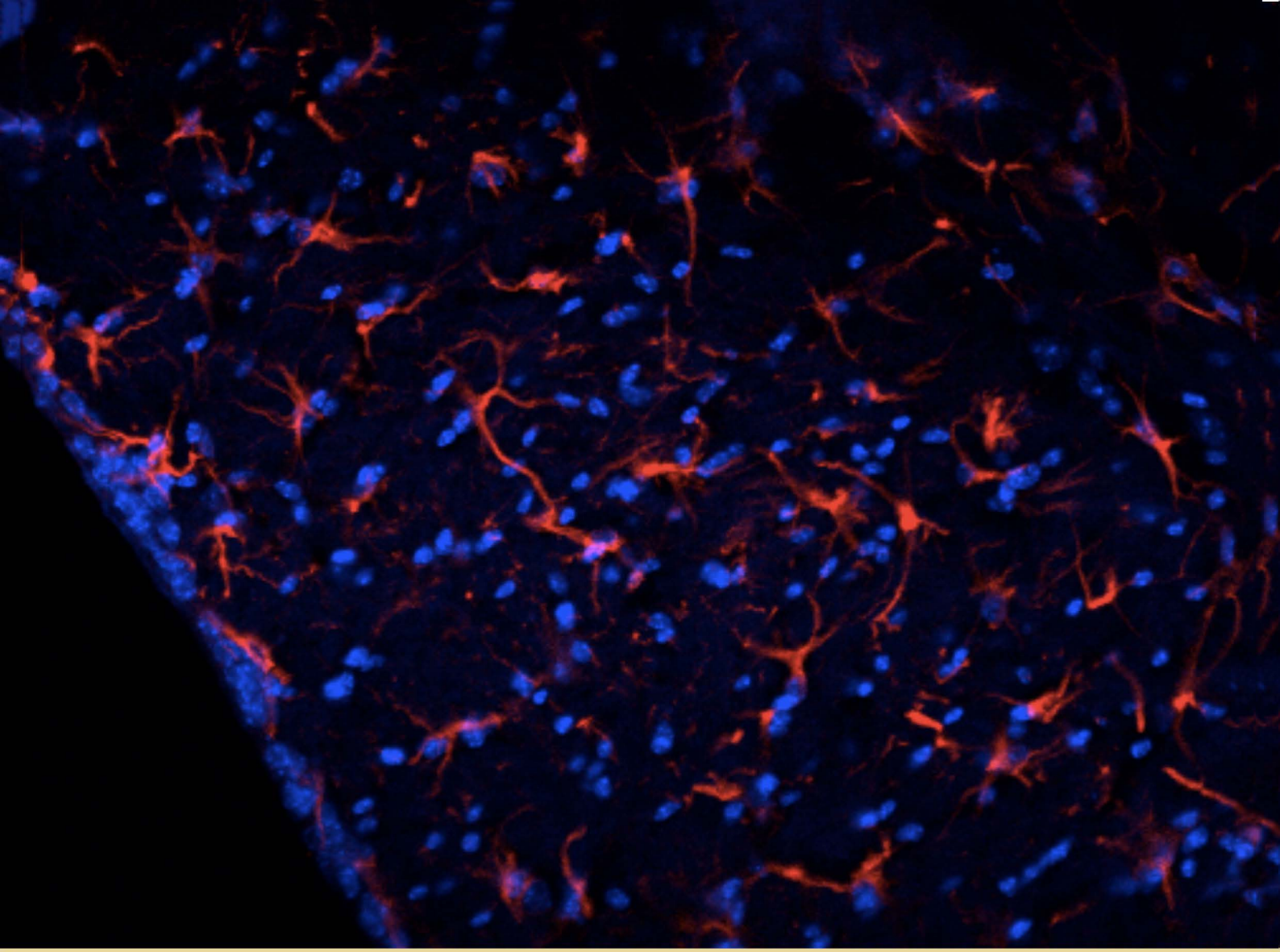

Sara Carolina de Carvalho Henriques

CHARACTERISATION OF A MULTIPLE SCLEROSIS ANIMAL MODEL – BEHAVIOUR AND BIOCHEMICAL EFFECTS OF CUPRIZONE INTOXICATION, IN A DPP-IV CENTRED APPROACH

Dissertação de Mestrado em Bioquímica, orientada pelo Doutor Flávio Reis e pelo Professor Doutor Paulo Santos, apresentada ao Departamento de Ciências da Vida da Faculdade de Ciências e Tecnologia da Universidade de Coimbra

Julho de 2016

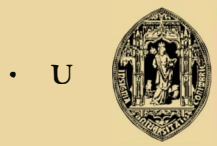

UNIVERSIDADE DE COIMBRA

Sara Carolina de Carvalho Henriques

CHARACTERISATION OF A MULTIPLE SCLEROSIS ANIMAL MODEL – BEHAVIOUR AND BIOCHEMICAL EFFECTS OF CUPRIZONE INTOXICATION, IN A DPP-IV CENTRED APPROACH

Dissertação apresentada ao Departamento de Ciências da Vida da Faculdade de Ciências e Tecnologia da Universidade de Coimbra para prestação de provas conducentes ao grau de Mestre em Bioquímica

Dissertation presented to the Department of Life Sciences from the Faculty of Science and Technology of the University of Coimbra as a requirement for the degree of MSc in Biochemistry

Coimbra, July 2016

· U C ·

UNIVERSIDADE DE COIMBRA

Cover illustration: *GFAP (red) in mice corpus callosum. Nuclei represented in blue (see p. 50).*

I had to find you
Tell you I need you
Tell you I set you apart

Tell me your secrets
And ask me your questions
Oh, let's go back to the start

(...)

I was just guessing
At numbers and figures
Pulling the puzzles apart

Questions of science
Science and progress
Do not speak as loud as my heart

Tell me you love me
Come back and haunt me
Oh, and I rush to the start

Running in circles
Chasing our tails
Coming back as we are

Nobody said it was easy
Oh, it's such a shame for us to part
Nobody said it was easy
No one ever said it would be so hard

I'm going back to the start

– Coldplay, The Scientist

Work conducted at the Laboratory of Pharmacology and Experimental Therapeutics, Institute for Biomedical Imaging and Life Sciences (IBILI) – Faculty of Medicine of the University of Coimbra (FMUC), Portugal, under the supervision of Flávio Reis, PhD, and Paulo Santos, PhD

This study was supported by Fundação para a Ciência e Tecnologia (FCT) through UID/NEU/04539/2013 (CNC.IBILI Consortium) and a research grant supported by Biogen.

ACKNOWLEDGMENTS

Ao Doutor Flávio Reis, um enorme agradecimento pela belíssima oportunidade que me deu de trabalhar no seu grupo de investigação, numa área que sempre me fascinou, as neurociências. Obrigada por todos os conselhos, apoio incondicional, pelos desafios lançados, sempre acompanhados por boa disposição. Obrigada pela amizade e espero ter estado à altura de um trabalho que tanto me desafiou e cativou.

Ao Dr. Filipe Palavra pela amizade, por todos os ensinamentos, empenho e disponibilidade, sem esquecer todos os momentos de diversão que trazia para o ambiente de trabalho, fossem baseados em piadas ou simplesmente nas músicas que todos gostamos (*Hello is there anybody in there?*).

Ao Professor Doutor Paulo Santos por me ter apoiado tanto quando mais precisei. Obrigada por toda a confiança depositada. Espero ter mostrado ser digna de toda a sua confiança e ajuda.

Ao Professor Doutor Frederico Pereira por todo o interesse mostrado, e por todas as sugestões e críticas que muito contribuíram para enriquecer e consolidar este trabalho.

À Sara Nunes, por me ter ensinado tanto durante este ano, por toda a ajuda (sobretudo a de última hora), e pelo pensamento crítico, que tanto ajudou à realização deste trabalho. Obrigada pela paciência e disponibilidade.

À Johanna Simões, a minha companheira de aventuras laboratoriais, um obrigada por ser uma aprendiz tão dedicada e incansável, por toda a ajuda e disponibilidade, por toda a alegria (e maluquices) que trouxe nos momentos de trabalho, pelo curativo improvisado e por fazer com que tudo estivesse *tranquilo* e *favorável*, mas mais que tudo, pela amizade!

Ao João Dinis, parceiro nas maratonas de testes comportamentais, na demanda de encontrar o *best mouse in the house*. Obrigada por toda a ajuda na análise dos vídeos e estatística, mas sobretudo pela amizade, companhia e momentos boa disposição nos testes com os ratinhos.

À Inês Pita, por todos os ensinamentos, ajuda e sobretudo paciência quando as coisas corriam menos bem.

Às Doutoras Raquel Santiago e Maria Madeira pela disponibilidade e ajuda na realização do estudo de expressão génica.

Aos meus colegas do Laboratório de Farmacologia e Terapêutica Experimental, Marina e José, pela amizade, companheirismo, espírito de entreajuda e sessões de gargalhadas.

Aos meus pais, a quem mais agradeço, por me terem dado tudo o que podiam e não podiam, por tanto terem investido e confiado nos meus sonhos. Por todas as vitórias que celebrámos juntos, mas sobretudo pelos momentos menos bons em que nunca me deixaram ir a baixo e que me fizeram ser mais forte. Amo-vos muito!

Ao Eduardo, o meu *Slytherin* bonzinho, por todo o amor e amizade (*infinitos inception*) ao longo destes anos. Por nunca me teres abandonado quando mais precisei, por me teres ajudado a erguer mesmo quando eu me dava por derrotada, pela paciência (que foi precisa muita!) e por teres acreditado sempre em mim.

Aos meus irmãos, Mafalda e Manel, os mais *chatos* do mundo (mas que eu não trocava por nada) por me fazerem rir por tudo e por nada e por todo o apoio.

À minha avó, por sempre ter feito de mim uma neta querida, e por todos os miminhos e apoios que só uma avó como tu pode dar.

À Titinha e ao Donald, por todas as conversas filosóficas e por desde cedo me terem ajudado a crescer.

À Mafalda, *my fellow Gryffindor*, pela a amizade partilhada há já 20 anos e por todos os momentos que passamos juntas. Que muitos mais anos estejam para vir em que olharemos para traz e diremos: *After all this time, Always*.

Ao Marcelo, pelas pausas partilhadas, conversas sobre tudo e nada, pelos conselhos científicos, mas essencialmente por ter feito um excelente trabalho a trocar os cabos do computador.

Aos meus amigos Químicos, Sónia Pedreiro, Lígia Carreira, Joana Silva, Wasina Fins, Alexandre Oliveira (*Xano*), Joana Couto e Renato Silva, por toda a amizade, conversas científicas e entreajuda ao longo destes anos.

E, por último, mas não menos importante, ao meus meninos: Rodolfo, Napoleão e Nina, por tornarem todos os meus dias mais sorridentes, por todo o amor e carinho, e pela companhia nas longas noitadas.

ABSTRACT

Introduction: Multiple sclerosis (MS) is a chronic inflammatory immune-mediated disease of the central nervous system mainly characterized by degeneration of neurons' myelin sheath (demyelination). Recently, it has been suggested that glucagon-like peptide-1 (GLP-1), one of the main substrates of dipeptidyl peptidase IV (DPP-IV), exerts neuroprotective and neurotrophic properties. However, changes on the DPP-IV–GLP-1 pathway remain to be characterized in MS, including in animal models of the disease, such as the cuprizone (CPZ)-induced demyelination mouse model.

Aims: This study aimed to characterize behaviour and biochemical profiles associated with CPZ-induced demyelination followed by spontaneous remyelination due to toxin withdrawal, focusing on markers of neurotoxicity, demyelination, inflammation and DPP-IV/GLP-1 pathway.

Methods: Two male C57BL/6 mice groups (n=10 each) were fed with an oral solution of CPZ (0.2%) during 5 weeks (W5); after that, half of them (n=10) were maintained on vehicle (water) for two more weeks (W7), which allowed the definition of two relevant milestones: W5 for the peak of demyelination and W7 for the early stage of spontaneous remyelination. A vehicle (water)-treated group was used as control (n=10 for each time-point). At weeks 5 and 7, animals were subjected to behaviour experiments (Y-maze, open-field and splash tests). Additionally, gene and/or protein expression of GFAP, myelin-PLP, TNF-α, IL-1β, DPP-IV, GLP-1 and GLP-1R was accessed in cerebellum (through RT-PCR and WB) and in corpus callosum samples (by IHC).

Results: Behavioural tests confirmed a depression-related behaviour (splash test) and a trend to changes on parameters of anxiety (open field test) in the CPZ-treated mice. Myelin-PLP expression was decreased in the cerebellum and corpus callosum of CPZ-treated mice at the peak of demyelination (week 5), when compared with the control animals; these changes were reversed at week 7 (early remyelination phase). The CPZ-induced animal model of MS was able to mimic the gliosis component of the disease, revealed by the significantly increased GFAP protein expression during the demyelination phase, with recovered values in the early remyelination phase. Furthermore, a reversible inflammatory process, revealed by the overexpression of the cytokines TNF-α and IL-1β at week 5 (peak of demyelination), was

observed in this model, with normalized values at week 7 (early remyelination). Lastly, although unchanged expression of DPP-IV and GLP-1 was found in the cerebellum of CPZ-treated mice in weeks 5 and 7, there was an overexpression of DPP-IV in the corpus callosum and a reduced expression of GLP-1R in the cerebellum at the peak of demyelination.

Conclusions: The behavioural and biochemical changes observed are consistent with the temporal profile of demyelination and remyelination processes in this animal model of MS. The pattern of DPP-IV, GLP-1 and GLP-1R expression in the cerebellum and in the corpus callosum maintains intact the possibility to use this pathway as an interesting and relevant therapeutic target in MS. Further studies are mandatory to complement our preliminary data.

Keywords: *multiple sclerosis, cuprizone mouse model, demyelination/remyelination, dipeptidyl peptidase IV, glucagon-like peptide-1*

RESUMO

Introdução: A esclerose múltipla (EM) é uma doença crónica inflamatória imuno-mediada do sistema nervoso central, caracterizada pela degeneração da bainha de mielina (desmielinização) dos neurónios. Recentemente, foi sugerido que o peptídeo semelhante a glucagon 1 (GLP-1), um dos principais substratos da dipeptidil peptidase IV (DPP-IV), exerce propriedades de neuroprotecção e neurotróficas. No entanto, alterações na via DPP-IV–GLP-1 permanecem por caracterizar na EM, incluindo em modelos animais da doença, como o modelo animal de desmielinização induzida por cuprizona (CPZ).

Objectivos: Este estudo teve como objectivo caracterizar os perfis comportamental e bioquímico associados a desmielinização induzida por CPZ e subsequente remielinização provocada pela remoção da toxina, com enfoque em marcadores de neurotoxicidade, desmielinização, inflamação e da via DPP-IV/GLP-1.

Métodos: Dois grupos de murganhos C57BL/6 machos (n=10 cada) foram alimentados com uma solução oral de CPZ (0,2%) durante 5 semanas (W5); seguidamente, metade dos animais (n=10) foram mantidos em tratamento com o veículo (água) durante mais duas semanas (W7), o que permitiu a definição de dois marcos temporais: W5 para o pico de desmielinização e W7 para a fase inicial de remielinização. Um grupo tratado com o veículo (água) foi usado como controlo (n=10 para cada tempo de estudo). Após 5 e 7 semanas, os animais foram sujeitos a ensaios de comportamento animal (testes *Y-maze, open field* e *splash*). Adicionalmente, a expressão génica e/ou proteica de GFAP, PLP-mielina, TNF-α, IL-1β, DPP-IV, GLP-1 e GLP-1R foi analisada em amostras de cerebelo (através de RT-PCR e WB) e de corpo caloso (por IHC).

Resultados: Os testes comportamentais confirmaram a existência de um comportamento do tipo depressivo (teste *splash*) e alterações nos parâmetros de ansiedade (teste *open field*) nos animais tratados com CPZ. A expressão da PLP-mielina diminuiu no cerebelo e no corpo caloso nos animais tratados com CPZ no pico de desmielinização (semana 5), quando comparada com os animais controlo; estas alterações foram revertidas às 7 semanas (fase de remielinização precoce). O modelo animal de EM induzida por CPZ mimetizou a componente gliótica da doença, revelada pelo aumento de expressão de GFAP durante a fase de desmielinização, com recuperação na fase de remielinização precoce. Para além disso, o modelo permitiu constatar a

existência de um processo inflamatório, revelado pela expressão elevada das citoquinas TNF-α e IL-1β, na semana 5 (pico de desmielinização), com valores normalizados às 7 semanas (fase precoce de remielinização). Por fim, apesar da expressão inalterada de DPP-IV e GLP-1 encontrada no cerebelo dos animais nas semanas 5 e 7, observou-se uma expressão elevada de DPP-IV no corpo caloso e diminuída de GLP-1R no cerebelo no pico de desmielinização.

Conclusões: As alterações comportamentais e bioquímicas observadas são consistentes com o perfil temporal dos processos de desmielinização e remielinização neste modelo animal de EM induzida por CPZ. O perfil de expressão de DPP-IV, GLP-1 e GLP-1R no cerebelo e no corpo caloso mantém intacta a possibilidade de usar esta via como um alvo terapêutico interessante e relevante na EM. Estudos posteriores são necessários para complementar esta informação preliminar.

Palavras-chave: *esclerose múltipla, modelo da cuprizona em ratinho, desmielinização/remielinização, dipeptidil peptidase IV, peptídeo semelhante a glucagon 1*

CONTENTS

LIST OF FIGURES

LIST OF TABLES

LIST OF ABBREVIATIONS

Ab	Antibody
AD	Alzheimer's disease
ADEM	Acute disseminated encephalomyelitis
AHL	Acute haemorrhagic leukoencephalitis
ANOVA	Analysis of variance
APC	Antigen-presenting cell
BBB	Blood-brain-barrier
CD	Cluster of differentiation
CNS	Central nervous system
CPZ	Cuprizone
CSPG	Chondroitin sulphate proteoglycans
DC	Dendritic cell
DIS	Dissemination of lesions in space
DIT	Dissemination of lesions in time
DMF	Dimethylfumarate
DMT	Disease-modifying therapy
DNA	Deoxyribonucleic acid
DPP-IV	Dipeptidyl peptidase IV
EAE	Experimental autoimune encephalomyelitis
EC	Enzyme commission
ECM	Extracellular matrix

GA	Glatiramer acetate
GIP	Glucose-dependent insulinotropic polypeptide
GFAP	Glial fibrillary acidic protein
GLP-1	Glucagon-like peptide-1
GLP-1R	Glucagon-like peptide-1 receptor
GM-CSF	Granulocyte-macrophage colony-stimulating factor
Ig	Immunoglobulin
IHC	Immunohistochemistry
IL-1β	Interleukin 1 beta
IFNβ	Interferons β
MAG	Myelin-associated glycoprotein
MBP	Myelin basic protein
MeOH	Methanol
MHC	Major histocompatibility complex
MOG	Myelin oligodendrocyte glycoprotein
MRI	Magnetic resonance imaging
mRNA	Messenger ribonucleic acid
NMO	Neuromyelitis optica
MS	Multiple sclerosis
NTZ	Natalizumab
OPC	Oligodendrocyte progenitor cell
PD	Parkinson's disease
(PDGFR)α	Platelet-derived growth factor receptor alpha
PLP	Proteolipid protein
PNS	Peripheral nervous system

PPMS	Primary progressive multiple sclerosis
RRMS	Relapsing-remitting multiple sclerosis
RT-PCR	Reverse transcription polymerase chain reaction
SAB	Spontaneous alternation behaviour
SPMS	Secondary progressive multiple sclerosis
T2DM	Type 2 diabetes mellitus
Th	T helper cell
TMEV	Theiler's murine encephalomyelitis virus
TNF-α	Tumour necrosis factor alpha
Treg	Regulatory T cell
VLA-4	Molecule α4-integrin
WB	Western blot

PART I

INTRODUCTION

Chapter 1
Multiple sclerosis

Multiple sclerosis (MS) is a chronic inflammatory disease of the central nervous system (CNS), triggered by an autoimmune response to self-antigens. It is correlated with lymphocytic infiltration across the blood-brain-barrier (BBB), which leads to degeneration of both the myelin sheath (demyelination), which is synthesised by oligodendrocytes, and the underlying axon, leading to the disruption of neuronal signalling. Initially, inflammation is transient and remyelination occurs, but it is not durable, meaning that the early course of the disease is characterized by episodes of neurological dysfunction that usually recover. However, over time lesions become dominated by widespread microglial activation associated with extensive and chronic neurodegeneration, leading to a progressive phase of the disease (Compston & Coles, 2008; Nylander & Hafler, 2012; Ransohoff *et al.*, 2015).

MS is part of a group of primary CNS inflammatory demyelinating diseases which also include other clinical entities, such as Devic's disease, also known as neuromyelitis optica (NMO), acute disseminated encephalomyelitis (ADEM) and ADEM's hyperacute variant, acute haemorrhagic leukoencephalitis (AHL) (Popescu & Lucchinetti, 2012).

1.1. Epidemiology and risk factors

Worldwide, approximately 2.5 millions of individuals are diagnosed with MS, being the most common demyelinating disease of the CNS in humans (Belbasis *et al.*, 2015; Dendrou *et al.*, 2015).

Prevalence varies considerably between countries, being highest in Europe (108 per 100,000 inhabitants) and North America (140 per 100,000), and lowest in sub-Saharan Africa (21 per 100,000) and east Asia (22 per 100,000) (Belbasis *et al.*, 2015; Dendrou *et al.*, 2015). In Portugal, the prevalence of the disease is ~50 per 100,000 inhabitants, which indicates that about 5,000 people have MS (Machado *et al.*, 2010).

MS usually begins in early adulthood, age between 20–40 years, with affected women outnumbering men 2:1, since immune-mediated diseases are more common in this gender. Despite 10–15% of cases occur in first-degree relatives of patients with MS, which indicates a genetic component of the disease, there is no interpretable pattern of inheritance (Ransohoff *et al.*, 2015). Genetic susceptibility is possibly conferred by major histocompatibility complex (MHC) molecules, which modulate the immune response (particularly autoimmunity) and cell-cell interactions (Hemmer *et al.*, 2006; Dendrou *et al.*, 2015; Ransohoff *et al.*, 2015; Yadav *et al.*, 2015). A recent analysis of gene expression in MS cortical lesions indicated the presence of genes associated with T helper 1 (Th1)/Th17-mediated inflammation, microglia activation, oxidative stress, and cell death/DNA damage as the molecular events responsible for demyelination and neurodegeneration (Fischer *et al.*, 2013).

The early hypothesis about the aetiology of MS suggested it to be infectious, vascular or metabolic, according to the predisposition of the patient (Ransohoff *et al.*, 2015). Environmental factors, which include diet, infectious agents (e.g. Epstein-Barr virus), environmental toxins (e.g. smoking), and latitude/sunlight (via vitamin D), can as well contribute to the development of the disease (Belbasis *et al.*, 2015; Grigoriadis & van Pesch, 2015). However, the causes of MS are still unknown and there are no well-established risk factors to assist disease prevention. Therefore, MS seems to be the result of interaction between genetic and environmental factors, which contributes to assign it the label of "complex disease" (Belbasis *et al.*, 2015; Ransohoff *et al.*, 2015).

1.2. Pathogenesis

MS pathological hallmarks consist in confluent demyelinating areas, called plaques, that indicate a loss of myelin sheaths and oligodendrocytes, by variable gliosis[1] and inflammation, and by relative axonal preservation (at least in the early beginning of the disease). These plaques' location, number, size, and shape vary greatly among MS patients. Lesions are distributed through the white and grey matter of the brain and spinal cord, and although axons and neurons are mostly preserved in early MS, on-going disease results in gradual neuroaxonal loss, which is correlated with patient disability and brain atrophy, accompanied by ventricular enlargement (Figure 1).

The evolution of MS lesions occurs differently whether it is in an early state, or in a chronic disease phase; within each phase, different types and stages of demyelinating activity are evident (Popescu & Lucchinetti, 2012; Popescu *et al.*, 2013; Dendrou *et al.*, 2015; Frischer *et al.*, 2015).

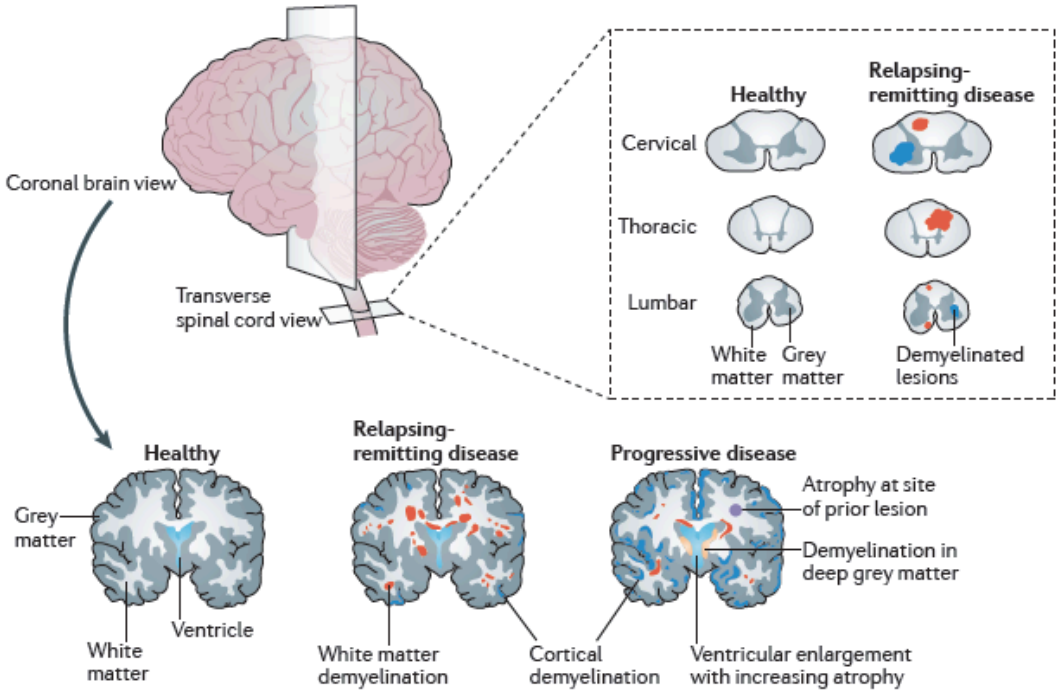

Figure 1. MS pathology. MS pathology is characterized by confluent demyelinated areas (plaques) in the white and grey matter of the brain and spinal cord, which indicate a loss of myelin sheaths and oligodendrocytes. Although axons and neurons are mostly preserved in early multiple sclerosis (relapsing-remitting disease), progressive disease results in gradual neuroaxonal loss that correlates with patient disability, and the brain atrophy that occurs is accompanied by ventricular enlargement (taken from Dendrou *et al.*, 2015).

[1] The proliferation and activation of glial cells (microglia, oligodendrocytes and astrocytes) in response to damage in the CNS.

Corpus callosum (Llufriu *et al.*, 2012) and cerebellum (Tornes *et al.*, 2014) are among the most affected areas of the CNS by this disease. Corpus callosum is responsible for connecting homologous regions of the left and right cerebral hemispheres of the brain, providing interhemispheric communication between cortical and subcortical neurons. It plays an important role in the organization of complex commands involving bilateral tasks with precise timing of information transfer between sides. Furthermore, it is the largest white matter structure in the brain, consisting of 200–250 million contralateral axonal projections. Lesions in this area provoke a bad connection between the two hemispheres, leading to a severe functional impairment (Llufriu *et al.*, 2012). In the other hand, cerebellum is responsible for the subject's motor control, and lesions affecting this structure are correlated with tremor and with severe loss of coordination (Tornes *et al.*, 2014).

1.2.1. General overview of CNS organization

Cells of the nervous system exhibit an extraordinary diversity in shape, size and number of unique interactions with other cells. The fundamental units consist of neurons and their axonal and dendritic processes embedded in a glial network providing additional structure and function. In different ways, macroglia (oligodendrocytes and astrocytes) and microglia also contribute to the cellular architecture of the CNS. Oligodendrocytes synthesize and maintain the myelin sheath that cover nerve fibres in white matter and allows saltatory conduction of the nerve impulse. Astrocytes provide architecture for neurons and define anatomical boundaries and also act as a source of growth factors and cytokines. Astrocytes assume many physiological roles including those necessary for conduction of the nerve impulse, and participate in the response to injury. On the other hand, microglia acts as the first and main form of active immune defence in the CNS.

Myelin is synthetized by mature oligodendrocytes, each of which contacts short segments of axons in CNS white matter. Defined growth factors regulate different processes of proliferation, migration and differentiation of oligodendrocyte precursors into myelinating cells. These glia cells elongate, making contact with nearby axons and forming a cup at the point of contact that encircles the axon; subsequently, it extends along the nerve fibre, creating an internodal myelinated segment. After maturation, between myelin segments (nodes of Ranvier) electrical resistance is low, thereby allowing depolarization, generating electrical

current, triggering saltatory conduction (Compston *et al.*, 2006; Compston & Coles, 2008). In addition to providing rapid saltatory conduction of action potentials, myelin provides axons a source of metabolites for their general wellbeing; indeed, chronic demyelinated axons are more prone to irreversible damage. Myelin is characterized by a high percentage of lipid (70–85%) and, consequently, a low percentage of protein (15–30%). Because of its high lipid content, these vesicles have the lowest intrinsic density of any membrane fraction of the nervous system. Proteins and lipids are asymmetrically distributed in this bilayer, with only partial asymmetry of the lipids. There are no "myelin-specific" lipids, but cerebroside (galactosyl ceramide)[2] is the most abundant, followed by cholesterol and phospholipids. There are also regional variations on the lipid-to-protein ratio; for example, myelin isolated from the spinal cord has a higher lipid-to-protein ratio than brain myelin from the same species. CNS myelin is produced by oligodendrocytes, while Schwann cells produce peripheral nervous system (PNS) myelin. The two types of myelin are chemically different, but they both perform the same function.

The absence of myelin in an axon has several consequences. It is suggested that nodal widening is sufficient to block conduction; in fact, the loss of myelin reduces the constraints on local current generated by the driving node (the last intact node before the demyelinated region) to act just at the localized (former) nodal membrane, but rather to become dissipated over a much larger area (Figure 2) (Compston *et al.*, 2006).

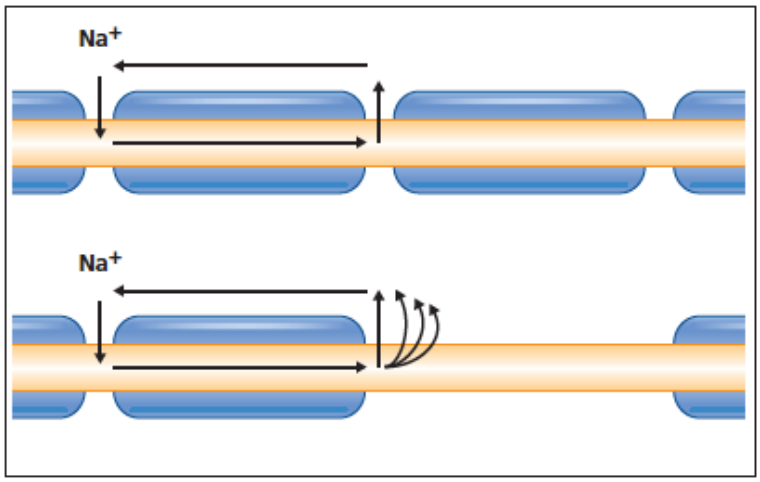

Figure 2. Flow of local action currents along a normal fibre (upper illustration) and one that has lost an internode of myelin (lower). Myelin normally helps to limit the flow of action current to the minimum portion of excitable axolemma at the node of Ranvier, but in the absence of myelin, the current becomes dispersed over a much larger area of axon membrane (taken from Compston *et al.*, 2006).

[2] Ceramide (family of lipid molecules) with a single sugar residue at the 1-hydroxyl moiety. The sugar residue can be either glucose or galactose; the two major types are therefore called glucocerebrosides and galactocerebrosides. Galactocerebrosides are typically found in neural tissue, while glucocerebrosides are found in other tissues.

1.2.2. Types of MS plaques

Based on a neuropathological study of a large collection of MS biopsies and autopsies, profound pathological heterogeneity of early active plaques, among different MS patients, was demonstrated. This suggests that the target of injury (myelin or oligodendrocytes) and the mechanisms of demyelination are distinctly different in subgroups of the disease and at different stages of disease development. Thus, MS lesions can be classified into four immunopatterns, based in specific myelin protein loss, plaque extent and topography, oligodendrocyte destruction, immunoglobulin deposition, and complement activation.

Patterns I and II (found in 15% and 58% of MS patients, respectively) share several similar features, with perivenous distribution of lesions, which, by confluence, result in large demyelinated plaques. Active demyelination is associated with a T-lymphocyte and macrophage dominated inflammation. The major difference between these two patterns is the prominent deposition of immunoglobulin (Igs; mainly IgG) and complement C9neo antigen at sites of active myelin destruction detectable in pattern II lesions. In pattern I lesions, the destructive process may be induced, mainly by products of activated macrophages.

In pattern III lesions (found in 26% of MS patients), demyelination is not centred on inflamed blood vessels. This pattern is defined by preferential myelin-associated glycoprotein (MAG) loss and massive oligodendrocyte apoptosis; since these are responsible for the axon myelination, remyelinated plaques are absent. This oligodendrocytes' disturbance is possibly a result of infection with a hitherto unknown virus or damage mediated by some unknown toxin.

Pattern IV lesions (found in 1% of MS patients) are associated with profound nonapoptotic death of oligodendrocytes in periplaque white matter.

The characterization of these different patterns helped understanding why a therapy that may be helpful for one group of patients, or at one stage of patient's disease, may be inefficient for another (Lucchinetti *et al.*, 2000; Popescu & Lucchinetti, 2012; Popescu *et al.*, 2013).

1.2.3. MS and inflammation

The BBB prevents the passage of most large molecules and cells, although specific vesicular and other transport mechanisms provide the brain with essential nutrients and permit a degree of cellular traffic. Lymphocyte penetration of cerebral vessels occurs through channels of endothelial cells and, thus, represents an active process mediated by endothelia[3]. This cellular migration is also dependent on modifications in the expression of cell surface molecules on activated T cells as well as endothelial cells, together with the secretion of enzymes that degrade the extracellular matrix in the subendothelial space. Clearly, the expression of these specific molecules responsible for immunological recognition alters under conditions of inflammatory cell activation, leading to an amplification of the steady-state cellular surveillance that occurs in health and contributing to the perivenular concentration of inflammatory cells that characterizes most demyelinating diseases. Thus, migration results from changes on endothelia and activated lymphocytes.

MS pathology seems to result from an immune-driven reaction to a myelin antigen; in fact, the trigger that sets off the disease has not been clearly identified. Although inflammation is present at all stages of MS, it is more pronounced in acute than in chronic phases. However, it is known that this disorder involves a cross-talk between the innate and adaptive immune systems. Macrophages account for the majority of the infiltrate, followed by $CD8^+$ T cells, whereas lower numbers of $CD4^+$ T cells, B cells and plasma cells can also be found.

During the establishment of central tolerance in the thymus, most autoreactive T cells are deleted; however, this process is imperfect, and some autoreactive T cells are released into the periphery. In a healthy individual, the maintenance of these cells is kept by peripheral tolerance through immunosuppressive mechanisms. If this tolerance is broken, through the reduced function of regulatory T (Treg) cells and/or the increased resistance of effector B cells and T cells to suppressive mechanisms, CNS-directed autoreactive B cells and T cells can be activated at the periphery to become aggressive effector cells by molecular mimicry, novel autoantigen presentation, recognition of sequestered CNS antigen released into the periphery or bystander activation.

Once peripherally activated, $CD8^+$ T cells, differentiated $CD4^+$ T Th1 and Th17 cells, B cells and innate immune cells can infiltrate the CNS, leading to inflammation and tissue

[3] Cells that lines the interior surface of blood vessels and lymphatic vessels, forming an interface between circulating blood or lymph in the lumen and the rest of the vessel wall.

damage, which is an essential step in the pathogenesis of MS. B cells trafficking out of the CNS can undergo affinity maturation in the lymph nodes before re-entering the target organ and promoting further damage (Figure 3).

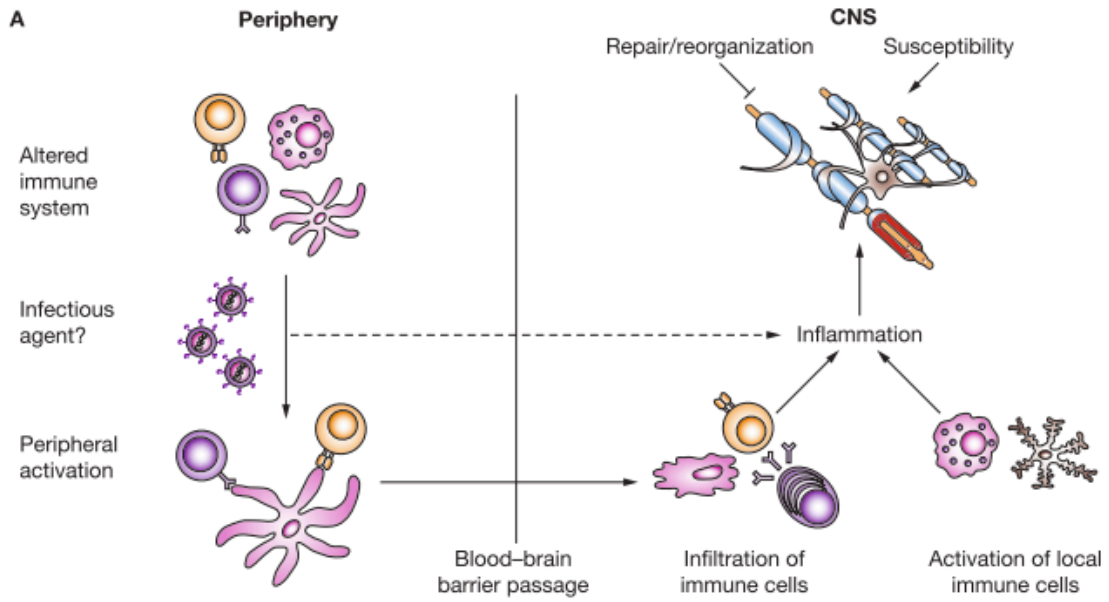

Figure 3. Pathogenetic concept for the development of MS. MS patients inherit traits that lead to an altered immune response. Activated antigen-specific T cells and B cells cross the BBB and target self-antigens expressed by oligodendrocytes and neurons. In concert with the innate immune response in the CNS, T cells and B cells cause inflammatory damage. Susceptibility of oligodendrocytes and neurons to inflammatory damage, and the capacity for CNS repair and reorganization determine the extent and functional consequences of the inflammatory damage (taken from Hemmer *et al.*, 2006).

Since demyelination is the main feature of MS neuropathology, it is probable that the main autoreactive targets are myelin protein-derived antigens. In fact, myelin basic protein (MBP), proteolipid protein (PLP) and myelin oligodendrocyte glycoprotein (MOG) have been demonstrated to be recognized by circulating $CD4^+$ T cells in both MS patients and healthy individuals.

In the experimental autoimmune encephalomyelitis (EAE) animal model (Chapter 2, Section 1), infiltrating $CD4^+$ T cells are re-activated in the CNS by antigen-presenting cells (APCs), including $CD11c^+$ dendritic cells (DCs), leading to monocyte recruitment into the CNS, as well as naive $CD4^+$ T cell activation through epitope spreading that further fuels the inflammation. In addition, both Th1/Th17 can potentiate neuroinflammation by secreting granulocyte-macrophage colony-stimulating factor (GM-CSF). This GM-CSF-only-producing Th cells were detected in MS and EAE. GM-CSF-only-producing Th cells and $CD11b^+$ $CD4^+$

T cells possess CNS-homing properties and are associated with autoimmune inflammation in MS/EAE.

$CD8^+$ T cells infiltrate the parenchyma and, as well as secreting inflammatory mediators, directly attack cells expressing human leukocyte antigen class I, such as neurons and oligodendrocytes. B cells are predominantly found in the perivascular space and meninges, where they release IgG antibodies, which bind to proteins expressed on the surface of oligodendrocytes and neurons. Bound antibodies can fix complement, thereby initiating the complement cascade or inducing antibody-mediated phagocytosis by macrophages. Activated macrophages also release inflammatory and toxic molecules (e.g. nitric oxide), which predominantly damage oligodendrocytes and neurons. Reactive astrocytes induce gliosis at the lesion border. Following the inflammatory damage, oligodendrocytes proliferate and remyelinate the demyelinated axons (Figure 4) (Compston *et al.*, 2006; Hemmer *et al.*, 2006; Dendrou *et al.*, 2015; Grigoriadis & van Pesch, 2015; Yadav *et al.*, 2015).

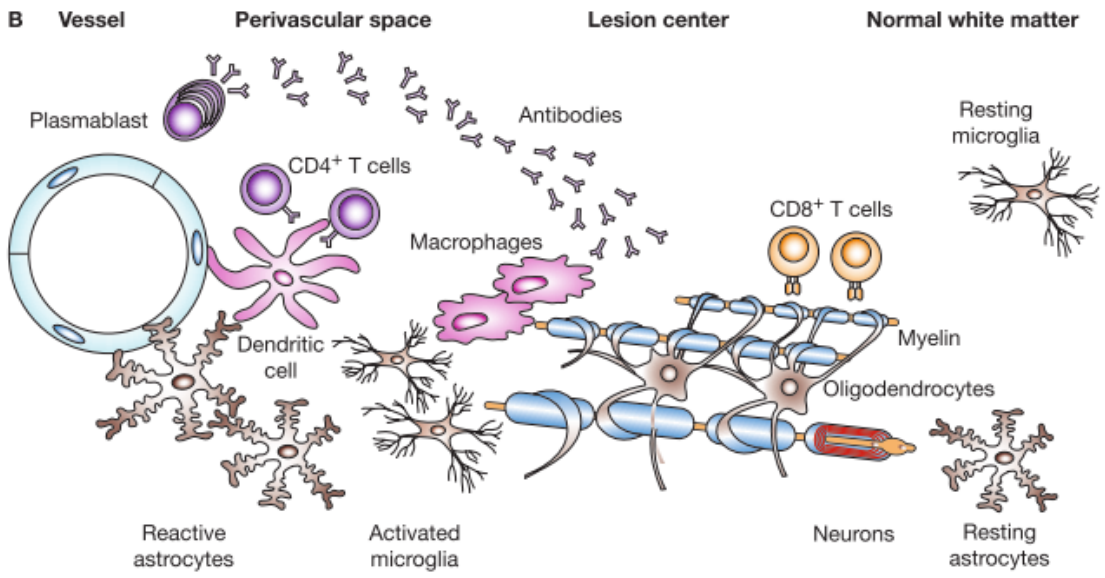

Figure 4. Immunopathogenesis of MS. T cells, B cells and macrophages infiltrate the lesion. $CD4^+$ T cells are located in the perivascular cuff. These cells become reactivated by antigens presented on dendritic cells and microglial cells, and locally release cytokines and other inflammatory mediators, thereby attracting macrophages to the lesions. $CD8^+$ T cells infiltrate the parenchyma and, as well as secreting inflammatory mediators, they directly attack cells expressing human leukocyte antigen class I such as neurons and oligodendrocytes. B cells are predominantly found in the perivascular space and meninges, where they release IgG antibodies. These antibodies bind to proteins expressed on the surface of oligodendrocytes and neurons. Bound antibodies can fix complement, thereby initiating the complement cascade, or inducing antibody-mediated phagocytosis by macrophages. Activated macrophages also release inflammatory and toxic molecules (e.g. nitric oxide), which predominantly damage oligodendrocytes and neurons. Reactive astrocytes induce gliosis at the lesion border. Following the inflammatory damage, oligodendrocytes proliferate and remyelinate the demyelinated axons (taken from Hemmer *et al.*, 2006).

1.2.4. Remyelination

Remyelination follows the pathological loss of myelin in diseases such as MS. This phenomenon consists in generating new myelin sheaths around the demyelinated axons in the adult CNS. This process can restore conduction properties to axons (thereby restoring neurological function) and it is believed to exert an important neuroprotective role on axons.

Remyelination occurs in many MS lesions, but becomes increasingly ineffective and eventually fails in the majority of lesions and patients. Efforts to understand the causes for this failure of regeneration have led research into the biology of remyelination and to the complex, interdependent cellular and molecular factors that regulate this process.

This mechanism occurs in two major phases. The first one consists of proliferation and migration into demyelinating lesions of oligodendrocyte progenitor cells (OPCs), which are widespread throughout the adult CNS (in both white and grey matter) and are capable of making and remodelling myelin throughout the lifespan; subsequently, OPCs must differentiate into mature myelinated oligodendrocytes, contacting, enwrapping and compacting around demyelinated axons to generate functional myelin sheaths.

These precursor cells could be isolated from an adult brain, identified by the presence of transcription factors, such as Olig2 and NKx2-2, as well as the surface markers platelet-derived growth factor receptor (PDGFR)α and NG2 (Chari, 2007; Palavra *et al.*, 2014; Harlow *et al.*, 2015; Keough *et al.*, 2016; Marinelli *et al.*, 2016).

The cause of remyelination failure is likely multifactorial and includes lesion- associated factors that impede any of the aforementioned steps. These inhibitory cues include Wnt and Notch signalling pathways, semaphorins, Lingo-1, myelin debris, as well as extracellular matrix (ECM) molecules such as hyaluronan and chondroitin sulphate proteoglycans (CSPGs). CSPGs act as guidance and signalling molecules during development, maintain the structural integrity of the healthy CNS in specialized structures, such as basement membranes, perineuronal nets and nodes of Ranvier. In the damaged CNS (such as in MS), CSPGs become highly upregulated as part of the astrogliotic scar, and are potent inhibitors of axon regeneration after traumatic injury (Keough *et al.*, 2016).

Still, remyelination pathways are not yet fully understood, but the comprehension of those could possibly lead to the discovery of new therapeutic targets. The study of these targets could be best performed using animal models of demyelination and demyelination.

1.3. Clinical features

1.3.1. MS forms and symptomatology

MS is characterized by two clinical phenomena – relapses and progression. Relapses are the clinical expression of the focal acute inflammatory demyelinating plaques distributed among the CNS. Clinical phenotypes are sorted based on the presence and timing of these two features (Frischer *et al.*, 2015; Paz Soldán *et al.*, 2015).

The majority of patients with MS (around 85%) initially have episodes of neurological dysfunction (the first of them is known as clinically isolated syndrome), followed by periods of stability (remission) (Figure 5). Relapses are associated with the appearance of new lesions or reactivation of old ones in the brain, brainstem and spinal cord. This stage is termed relapsing-remitting MS (RRMS) and, in clinical terms, it can range from no persistent neurological deficits between relapses to recurrences that later in time leave some neurological discapacity.

Initial symptoms include paralysis, sensory disturbance, weakness or diminished dexterity in one or more limbs, lack of coordination, monocular visual loss (optic neuritis), double vision (diplopia), gait instability, and ataxia. Clinical symptoms may vary according to the site of lesions, likewise, as the disease progresses they tend to aggravate and several neurological signs and symptoms can typically be found in later stages of the disease: bladder dysfunction, fatigue, heat sensitivity (the Uhthoff phenomenon [4]); ancillary symptoms: Lhermitte's sign[5], hemifacial weakness or pain, vertigo, and brief tonic spasms; cognitive deficits: memory loss, impaired attention, problem-solving difficulties, slowed information processing, and difficulties in switching between cognitive tasks; and depression (Hauser & Oksenberg, 2006; Compston & Coles, 2008).

Within about 12 years, approximately 40% of the patients with RRMS enter a phase of uninterrupted disease progression, which is known as secondary progressive MS (SPMS). These patients undergo an important atrophy of the CNS, with decreased brain volume and increased axonal loss. However, in around 15% of the cases this clinical disability begins with a progressive character, defining the primary-progressive phenotype of the disease (PPMS). This is characterized by gradual neurological dysfunction normally without exacerbations (Figure 5). Instead of what happens with the most common MS form, PPMS affects more the

[4] Transient worsening of symptoms and signs when core body temperature increases, such as after exercise or a hot bath.

[5] An electric shock-like sensation down the spine and into the limbs evoked by neck flexion.

male gender and the spinal cord is more frequently involved (Compston *et al.*, 2006; Compston & Coles, 2008; Cohen & Rae-Grant, 2010; Dendrou *et al.*, 2015; Iwanowski & Losy, 2015; Paz Soldán *et al.*, 2015). Patients with PPMS most likely present pattern IV lesions in the CNS (Lucchinetti *et al.*, 2000).

Inflammatory mechanisms dominate in the early phases of the disease (RRMS), but the development of a more progressive clinical phenotype, such as a SPMS (or inclusively PPMS) is due to neurodegeneration. As previously explained, during the earlier stage of the disease, mechanisms of repair (remyelination) occur, but over time they become insufficient to compensate for on-going damage, resulting on permanent disability (Cohen & Rae-Grant, 2010). So, disease-modifying therapies (DMTs) have only shown efficiency in RRMS, having little or no beneficial effects in SPMS or PPMS due to those different immunological and pathophysiological mechanisms involved (Iwanowski & Losy, 2015).

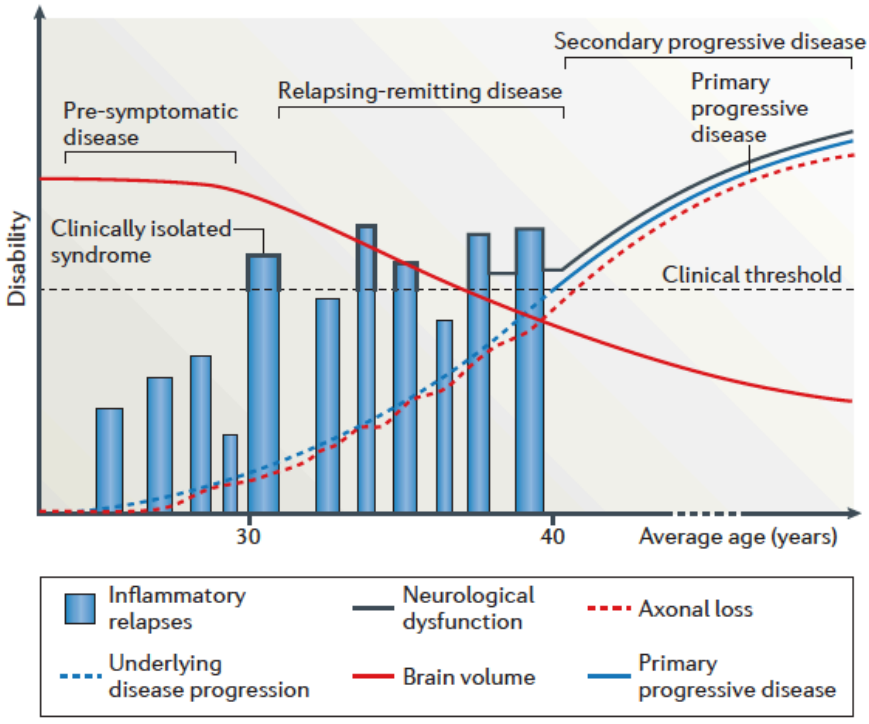

Figure 5. MS clinical course. MS has a heterogeneous course. The most common form (affecting ~85% of patients) is RRMS characterized by an initial episode of neurological dysfunction (clinical isolated syndrome), followed by a remission period of clinical recovery, and then recurring episodes of relapse and remission (black line). Within ~12 years, ~40% of the patients with RRMS enter a phase of uninterrupted disease progression, known as SPMS. These patients undergo an important atrophy of the CNS, with decreased brain volume (red line) and increased axonal loss (pointed red line). In ~15% of the cases this clinical disability begins with a progressive character, PPMS (blue line). This is characterized by gradual neurological dysfunction with an absence of relapses (taken from Dendrou *et al.*, 2015).

1.3.2. Diagnosis and prognosis

Diagnostic criteria for MS include clinical and paraclinical laboratory assessments emphasizing the need to demonstrate dissemination of lesions in space (DIS) and time (DIT) and to exclude alternative diagnoses. Although the diagnosis can be made on clinical grounds alone, magnetic resonance imaging (MRI) of the CNS can support, supplement, or even replace some clinical criteria, as most recently emphasized by the McDonald Criteria of the International Panel on Diagnosis of MS 2010. McDonald Criteria have resulted in earlier diagnosis of MS with a high degree of both specificity and sensitivity, allowing for better counselling of patients and earlier treatment (Polman *et al.*, 2011).

Many people with newly diagnosed or early-stage MS are overwhelmed by the uncertain prognosis, since there's no currently cure for the disease (Wingerchuk & Carter, 2014). However, MS patients, despite the limitations induced by the disease, can have the same life expectancy as the general population. Symptoms of the disease can cause pain, discomfort and inconvenience, even though most patient will never become severely disabled.

In addition, recent studies suggest PPMS portended a worse prognosis than RRMS or even SPMS (Paz Soldán *et al.*, 2015).

1.3.3. Disease-modifying therapies

Infiltration of immune cells from the periphery has been the main target of currently available therapies for MS. Although these broad-spectrum immunomodulatory drugs reduce immune cell activity and entry into the CNS and decrease relapse frequency, they are often associated with side effects (Dendrou *et al.*, 2015).

Since there is no cure for MS, current preventive DMTs have been used as the main therapeutic strategy. These have shown to affect the course of MS by reducing the frequency and severity of relapses and delaying progression of disability to some degrees. DMTs can be divided in two groups: first- and second-line DMTs.

First-line agents act at the inflammatory course of the disease (immunomodulators) with a good safety profile. There are four classes of DMTs available as first-line therapies for RRMS patients: interferons β 1a (IFNβ-1a) and 1b (IFNβ-1b) and glatiramer acetate (GA), both injectable and available for more than 15 years, and teriflunomide and dimethylfumarate

(DMF), newcomer oral DMTs. IFNβs have a limited capacity to reduce the number of circulating lymphocytes. Both IFNβ-1a and IFNβ-1b are considered safe injectable therapeutic options with limited drug interactions. The most frequent adverse events of IFNβ treatment are benign but annoying flu-like symptoms (30 – 60% of patients) that can be relieved by the use of nonsteroidal anti-inflammatory drugs, such as ibuprofen. GA is an immunomodulatory agent and a synthetic peptide made of four distinct aminoacids randomly assembled: Glutamic acid, Lysine, Alanine and Tyrosine. GA does not affect the number of circulating lymphocytes, such as IFNβs, but switches lymphocyte polarization from a pro-inflammatory Th1 to an anti-inflammatory Th2 profile. Teriflunomide is an inhibitor of pyrimidine synthesis capable or reducing the number of circulating leukocytes. DMF is an oral immunomodulatory drug with the capacity to reduce the number of circulating lymphocytes and to promote the synthesis of anti-inflammatory proteins and mediators, which, in a global perspective, allow cells to survive within an inflammatory milieu (Aharoni, 2010; Wingerchuk & Carter, 2014; Michel *et al.*, 2015).

Second-line drugs, which include natalizumab (NTZ), fingolimod and alemtuzumab, are agents that have proven therapeutic superiority to first-line agents, however, they are associated with significant side effects. NTZ is a synthetic monoclonal antibody (Ab) directed against the adhesion molecule α4-integrin (VLA-4). It has no significant drug interactions, but should not be used in combination with other DMT or immunosuppressors. NTZ is associated with a non-negligible risk (overall risk of 1/200) of serious infections, namely with progressive multifocal leukoencephalopathy, caused by JC virus. Fingolimod is a sphingosine-1-phosphate receptor agonist and a generally well-tolerated oral DMT. This drug reduces the number of circulating lymphocytes; however, it can present some serious side effects, such as cardiac, hepatic, infectious and ocular complications. Alemtuzumab is a monoclonal Ab directed against CD52. This drug is associated with infusion reactions in virtually all patients. Slow (over 4 h) infusion and premedication with methylprednisolone for the initial 3 days of each course of treatment, and with acetaminophen and diphenhydramine, is recommended to decrease the severity of these infusion reactions. Most patients will develop antibodies against alemtuzumab without any observed clinical impact.

Decisions to consider the best therapeutic plan for each MS patient are based on past and current disease activity. The efficacy of DMTs is limited to the relapsing clinical course of MS. In progressive forms of MS these drugs are partially or totally ineffective. Important questions remain about the right timing to switch for a second-line agent and whether escalating therapy is an appropriate strategy. There are two contrasting treatment strategies when initiating

treatment with DMTs in MS: escalation and induction therapy. Escalation therapy consists of early start first line DMTs. If first line DMTs are ineffective or partially effective, on-going therapy is switched to second line drugs. Induction therapy supports the early use of immunosuppressive drugs followed by long-term maintenance treatment, generally with the use of immunomodulatory agents (Aharoni, 2010; Wingerchuk & Carter, 2014; Fenu *et al.*, 2015; Michel *et al.*, 2015).

Recently, an experimental study described a new drug candidate, fluorosamine, that promotes OPC growth by inhibiting CSPG synthesis, allowing remyelination following focal demyelination in mice (Keough *et al.*, 2016). Further studies (clinical trials) should be performed to test the efficiency and safety of this new drug in humans. These results are encouraging, since they present remyelination as a new possible pharmacological target for MS treatment, and possibly more efficient and with less side effects.

Nevertheless, MS is still a disease without a totally efficient treatment. Existing DMTs only act by preventing disease's symptoms, not actually curing it; furthermore, many forms of the disease, which are also the most severe, are still practically untreatable. Hence, there's an urgent need to deeply study and understand this disease, which considerably varies between patients. However, the human CNS is of difficult access, and can only be monitorized by non-invasive techniques or in a post-mortem examination. Therefore, the study of animal models is the key to fully understand this disease and to approach future treatments.

Chapter 2
Animal models of MS

MS involves a complex interaction between two of the most intricate biological systems, the immune system and the CNS; furthermore, mechanistic studies in this disease are difficult since CNS tissue is arduous to access and immune responses within this tissue cannot be easily monitored. Hence, animal models have been crucial for addressing MS pathogenesis, and to mimic the different clinical and pathological aspects of the disease (Ransohoff, 2012; Star *et al.*, 2012; Simmons *et al.*, 2013).

Since MS is such a complex and exclusively affecting humans' disease, there is not a single animal model that can capture the entire spectrum of its heterogeneity and variety in clinical and radiological manifestations. Nevertheless, these models have been continually refined, approaching more and more the reality of the human disease. Therefore, MS animal models have been critical for increasing our knowledge of the disease, such as the development of new therapeutic approaches (Denic *et al.*, 2011; Simmons *et al.*, 2013; Ransohoff *et al.*, 2015).

The most widely used models are experimental autoimmune encephalomyelitis (EAE) model; viral-induced models, mainly Theiler's murine encephalomyelitis virus (TMEV) infection and consequential chronic demyelination; and toxic-induced models of demyelination, including the cuprizone (CPZ) model and focal demyelination induced by lyso-phosphatidylcholine (lysolecithin) (Torkildsen *et al.*, 2008; Mix *et al.*, 2010; Denic *et al.*, 2011; Star *et al.*, 2012).

2.1. Experimental autoimmune encephalomyelitis

EAE, developed in the 1930s, is the most widely studied animal model of MS. This model unveils quite well the inflammation process in the brain, being very helpful and used to model inflammatory aspects of the disease (Mix *et al.*, 2010).

EAE can be induced either by immunization with myelin antigens (active induction) or by adoptive transfer of activated T cells isolated from animals immunized with myelin antigens (passive induction). The immunization protocols activate primarily the $CD4^+$ T cells. Initial murine EAE models were developed in B10.PL or PL/J mouse strains, in which an epitope of myelin basic protein (MBP)1–11 is targeted, as well as in SJL mice in which encephalitogenic T cell responses to both MBP and proteolipid protein (PLP) are generated. Afterwards, C57BL/6 mice (also known as Black 6) were discovered to be susceptible to EAE via immunization with a peptide from myelin oligodendrocyte glycoprotein (MOG), being an extensively used animal model nowadays, mainly to exploit the many genetic models on the C57BL/6 background. In all of these models, inflammation predominantly targets the spinal cord, and mice develop subsequent symptoms of ascending flaccid paralysis. Thus, although these models have provided many insights into CNS autoimmune disease, the relative lack of involvement of the brain is a distinct difference from most patients with MS (Mix *et al.*, 2010; Ransohoff, 2012; Simmons *et al.*, 2013; Dendrou *et al.*, 2015; Procaccini *et al.*, 2015).

2.2. Toxic models of demyelination and remyelination

As mentioned before, the EAE model has been well established to mimic human disease and related pathology, but this model is still incomplete and lacks certain elements of the human disease. Moreover, EAE is the most commonly used model to study the autoimmune process in MS; therefore, other types of animal models for demyelination have been developed and used to supplement tool kits for studying human pathology and enhance development of more effective drugs. Toxic demyelination models are the most suitable to study those processes involved in spontaneous demyelination processes and neural repair (Ransohoff, 2012).

CPZ treatment is the most frequently used among the toxicant-induced MS models (which also include lysolecithin and ethidium bromide) and it has been used to study mechanisms of oligodendrocyte turnover, astrogliosis, and microgliosis. Unlike other toxicant-induced models, which are introduced in the brain by stereotaxic microinjections and result in focal demyelination, oral administration of cuprizone produces a global insult (Procaccini *et al.*, 2015).

2.2.1. The cuprizone model

CPZ, or bis(cyclohexanone)oxaldihydrazone, or N,N'-bis(cyclohexylideneamino)oxamide (IUPAC name) (Figure 6), is a selective and sensitive copper chelating agent. CPZ has peculiar neurotoxic properties when orally administered in mice, triggering rapid demyelination and gliosis, or rapid proliferation of glia subtypes. The mechanism of action has not yet been fully elucidated due to lack of structural information, but it is proposed that CPZ's neurotoxic activity is due to specific alterations in the brain copper metabolism, targeting mature oligodendrocytes. Copper is an essential element for the function of several metalloproteases, and decreased levels are observed in a number of degenerative disease. The CPZ mouse model captures several aspects of MS pathology, bypassing autoimmunity; so, it can be considered a good model for progressive forms of MS.

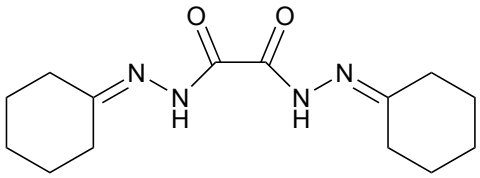

Figure 6. Cuprizone (CPZ) molecular structure. CPZ ($C_{14}H_{22}N_4O_2$) has a molecular weight (MW) of 278.35 g/mol, owns 2 H donors (N-H-), 4 H acceptors (=N-, =O), 2 routable bonds (N-N(H)) and 0 formal charge. CPZ has a partition-coefficient octanol/water slightly high (logP=1.6) and it is slightly soluble in water and extremely soluble in ethanol. It must be stored at 2-8ºC of temperature. When heated to decomposition emits toxic fumes of NO_x.

Different rodent strains react in distinct ways to CPZ, and the model is best characterized in the C57BL/6 strain that, unlike other strains, don't present a delayed or incomplete demyelination in certain areas of the brain, following CPZ treatment. Additionally, several studies concluded that female mice are more resistant to toxic demyelination induced by CPZ; so, typically, only male C57BL/6 mice are used as MS models induced by CPZ treatments,

which leads mainly to selective oligodendrocyte death and reproducible demyelination in the brain (Torkildsen *et al.*, 2008; Kipp *et al.*, 2009; Benetti *et al.*, 2010; Acs & Kalman, 2012).

Male C57BL/6 mice at 6 to 9 weeks of age, which are fed a diet of chow or water mixed with 0.2% CPZ, exhibit, by the third week of CPZ ingestion, reactive gliosis accompanied by oligodendrocyte apoptosis. Demyelination is evident after 4–6 weeks of intoxication in multiple structures that include the hippocampus, external capsule, rostral cerebellar peduncles, cerebellum, cerebral cortex and the most studied structure, the corpus callosum. This continued ingestion of the cooper-chelating agent results in white matter pathology similar to the pattern III MS lesions. As previously referred, this pattern is distinguished from the others by displaying extensive macrophage/microglia activation accompanied by oligodendrocyte apoptosis. When mice return to a normal diet (without CPZ), spontaneous robust remyelination occurs, which reaches completion by 2–5 weeks after the toxicant is withdrawn (Steelman *et al.*, 2012). While the majority of studies have been performed in the corpus callosum, other affected structures, such as cerebellum, remain practically unstudied in this animal model.

Moreover, several behaviour aspects are still to be characterized, brain imaging studies are lacking and many aspects related to gene and protein expression in different brain regions are still to be clarified. This is a versatile animal model of MS that has an interesting potential in research and whose knowledge clearly needs to be deepened.

Chapter 3
Dipeptidyl peptidase IV / GLP-1 pathway

Dipeptidyl-peptidase IV (DPP-IV) is a glycoprotein expressed in a vast variety of tissues. It is most well known by its expression and activity at intestine and pancreatic levels, being responsible in maintaining physiological glucose homeostasis, mainly due to the regulation of incretin hormones levels (Röhrborn *et al.*, 2015). Consequently, DPP-IV overexpression has been associated with type 2 diabetes mellitus (T2DM) and obesity, and the development of inhibitors for this protein has been a therapeutic strategy for the treatment of T2DM (e.g. sitagliptin) (Kazafeos, 2011). However, DPP-IV activity is not exclusive to the intestine and pancreatic β cells, since the enzyme is also expressed in several other tissues, including the brain, although its precise effects remain to be elucidated (Hölscher, 2012, 2014).

3.1. Structural properties and expression of DPP-IV

DPP-IV is a member of the S9b serine protease family, which also includes other three structurally homologous enzymes, DPP-VIII, DPP-IX and fibroblast activation protein (FAP) (Röhrborn *et al.*, 2015). This family of enzymes has rare substrate specificity, cleaving N-

terminal dipeptides from regulatory factors containing either L-proline or L-alanine in the penultimate position, inactivating or generating biologically active peptides.

DPP-IV, also known as adenosine deaminase complexing protein 2, T cell activation antigen CD26 and IUBMB Enzyme Nomenclature EC 3.4.14.5, is the best-characterized and most extensively studied member of the S9b family. DPP-IV is a ubiquitously expressed transmembranar glycoprotein of 110 kDa and 766 aminoacids, with 6 of them in the cytoplasm, 22 residues spanning the plasma membrane and 738 aminoacids comprising the extracellular domain (Figure 7). Unlike classical serine protease, the catalytic triad of Ser, Asp and His, is found in the C-terminal region of the enzyme in reverse order (Lambeir *et al.*, 2003; Rasmussen *et al.*, 2003; Röhrborn *et al.*, 2015). The principal role of DPP-IV is its enzymatic function. It has many physiological relevant substrates such as chemokines, regulated on activation normal T cell expressed and secreted (RANTES or CCL5), eotaxin, macrophage-derived chemokine, neuropeptides (such as neuropeptide Y [NPY] and substance P), and vasoactive peptides. It is responsible for the metabolic cleavage of certain endogenous peptides. Besides the peptidase activity, DPP-IV also functions as an adenosine deaminase binding protein and contributes to extracellular matrix binding.

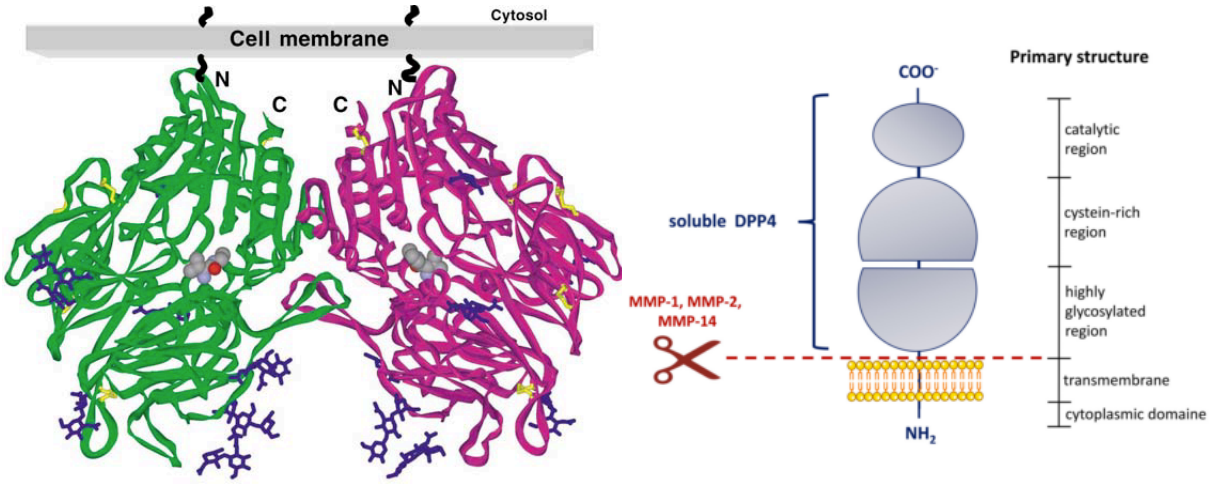

Figure 7. DPP-IV structure. *Left:* DPP-IV forms a homodimer (subunit A shown in green and subunit B in magenta). Each subunit consists of two domains: an α/β-hydrolase domain and a β-propeller domain. The full-length DPP-IV is a type II transmembrane protein in which amino acids 7–28 constitute the membrane-spanning region. The α/β-hydrolase domain, located closest to the membrane, consists of amino acids 39–51 and 506–766, and contains the active triad Ser630, Asp708 and His740. Residues 55–497 form the eight-bladed β-propeller domain. The inhibitor Val-Pyr is shown in CPK and coloured by element: carbon (grey), nitrogen (blue) and oxygen (red) (taken from Rasmussen *et al.*, 2003). *Right:* Schematic representation of the membrane-bound DPP-IV monomer. The extent of the circulating and soluble form of DPP-IV is illustrated on the left in blue. The shedding of DPP-IV from the membrane by indicated matrix metalloproteinases is shown by a scissor symbol in red. The vertical black bar on the right represents the primary structure with the delineation of the different regions. In green are interactions collected, which occur in the indicated region of the DPP-IV structure. MMP, matrix metalloproteinase; M6P/IGFII, mannose-6 phosphate/insulin-like growth factor 2 (taken from Röhrborn *et al.*, 2015)

DPP-IV is expressed on epithelial and endothelial cells of a variety of different tissues, such as intestine, liver, lung, kidney, brain and placenta. In the kidney, where the enzyme is exceptionally concentrated, DPP-IV is located in the cortex and found in the brush border and microvillus fractions. Furthermore, DPP-IV is also expressed on circulating T-lymphocytes and exists as a soluble circulating form in plasma and semen. While the soluble form has similar structure and function to the membrane bound form of the enzyme, it however lacks the hydrophobic transmembrane domain (Lambeir *et al.*, 2003).

3.2. DPP-IV/GLP-1 pathway – from diabetes to neurodegenerative disorders

DPP-IV is important in maintaining physiological glucose homeostasis, being responsible for the cleavage of two N-terminals of peptide hormones glucagon-like peptide-1 (GLP-1) and glucose-dependent insulinotropic polypeptide (GIP) in plasma, thus inactivating their insulinotropic activities (Kazafeos, 2011; Ezcurra *et al.*, 2013).

When moving through the intestine, nutrients interact directly with sensory receptors, integral membrane channel and transporter proteins localized on the microvillusrich apical membrane surface of endocrine cells. These cells are embedded in the mucosal lining through different regions of the intestinal tract and are responsible for the incretins' release upon nutrient stimulation. GLP-1 (a 31-aminoacid hormone) is produced by and secreted from enteroendocrine L-cells, by posttranslational cleavage of the 160-aminoacid proglucagon precursor protein, a process requiring prohormone convertase-1/3, and its biologically active forms are GLP-1 (7-36) amide and GLP-1 (7-37). GIP is produced in the K-cells, and is the single peptide (a 42-aminoacid hormone) derived from proteolytic processing of a 153-aminoacid precursor protein (Figure 8). Whereas GIP secreting K-cells are predominantly located in the duodenum and proximal jejunum, being exposed to nutrients soon after food ingestion, GLP-1 secreting L-cells are located more distally, in the distal ileum and colon, so it's secretion may be influenced by slowly digested macronutrients and products of bacteria fermentation (Drucker, 2006; Seino *et al.*, 2010; Kazafeos, 2011; Campbell & Drucker, 2013; Ezcurra *et al.*, 2013; Seino & Yabe, 2013).

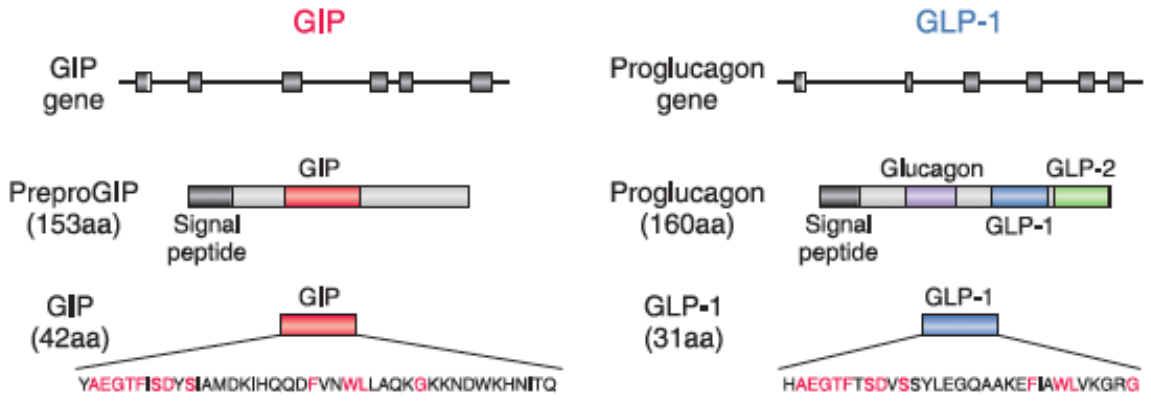

Figure 8. GIP and GLP-1 gene and structure. The glucose-dependent insulinotropic polypepide (GIP) gene is localized on human chromosome 17q21.3–q22 and comprises 6 exons. Proteolytic processing of preproGIP generates GIP that is secreted from K cells. The proglucagon gene is localized on human chromosome 2q36–q37 and comprises 6 exons. In the intestine, proteolytic processing of proglucagon generates glucagon-like peptide (GLP)-1 and GLP-2, whereas glucagon is produced in the pancreas (taken from Seino *et al.*, 2010).

Plasma levels of GLP-1, such as those of GIP, increase within minutes of eating; both hormones are potent simulators of insulin secretion. In fact, more than 2/3 of insulin normally secreted, during a meal, is due to insulinotropic actions of GLP-1 and GIP, but their activity is quickly abolished by DPP-IV–mediated truncation.

Upon released into circulation in response to intraluminal nutrients, these two primary incretin hormones act directly on pancreatic islets to enhance postprandial insulin secretion from pancreatic β cells. Within the pancreas, GLP-1 and GIP promote β cell proliferation and inhibit apoptosis, thereby expanding pancreatic β cell mass, while GIP enhances postprandial glucagon response and GLP-1 suppresses it. Both GLP-1 and GIP are ligands that bind to specific G protein-coupled receptors present in plasma membrane, the GLP-1 receptor (GLP-1R) and the GIP receptor (GIPR), respectively. Receptor binding activates an intracellular signalling cascade which will lead to the release of insulin.

Mice lacking the gene for DPP-IV show enhanced insulin secretion and accelerated clearance of blood glucose, partly because of increased endogenous levels of active GLP-1 and GIP. These results, and the recognition of the existence of an incretin defect in diabetic patients, lead researchers and pharmaceutical companies to search for drugs able to enhance incretins activity. The incretin-based therapies, a new class of antidiabetic drugs currently available for the treatment of diabetic patients, include DPP-IV inhibitors (such as sitagliptin) and GLP-1R agonists (namely exenatide).

As mentioned before, DPP-IV has several different substrates, each of them with distinct physiological roles. RANTES recruits leukocytes into inflammatory sites and is cleaved by DPP-IV. Elevated serum levels of RANTES in T2DM are associated with post-prandial

hyperglycemia. Insulin is also involved in suppressing the inflammatory process not only through preventing hyperglycaemia, but also by modulating key inflammatory molecules. In diabetic conditions the proinflammatory cytokines, such as interleukin-1 beta (IL-1β), interferon gamma (IFN-γ), and tumour necrosis factor alpha (TNF-α), inhibit glucose-stimulated insulin secretion and proliferation of β cells. Likewise, GLP-1R expression is widely detected in various cells and organs beyond pancreatic beta-cells, e.g. kidney, lung, heart, hypothalamus, endothelial cells, neurons, astrocytes, and microglia, suggesting that GLP-1 might have additional roles other than glucose lowering effects. GLP-1 is associated with anti-inflammatory properties in several tissues including in pancreatic islets and adipose tissue, contributing to lowering glucose levels in T2DM. In addition to these tissues, emerging data suggest that GLP-1-based therapies also showed anti-inflammatory effects on the liver, vascular system (including aorta and vein endothelial cells), brain, kidney, lung, testis, and skin by reducing the production of inflammatory cytokines and infiltration of immune cells in the tissues. Furthermore, the glia may play a critical role in the CNS inflammatory responses, and GLP-1R expression was found in astrocytes and microglia.

T2DM is a chronic and multifactorial metabolic disease characterized by a progressive β cell failure, leading to relative insulin deficiency, decreased insulin action and insulin resistance (Röhrborn *et al.*, 2015). These mechanisms contribute to hyperglycaemia and hyperlipidaemia, which cause glucotoxicity and lipotoxicity in other organs and tissues, including in the brain, thus increasing the risk for neurodegeneration/neuronal death, and functional and structural brain changes, culminating in cognitive dysfunction that underlies some dementia-type disorders (Duarte *et al.*, 2013).

3.3. DPP-IV/GLP-1 pathway in neurodegenerative diseases

Despite their most well-known effects occur in the intestine and pancreatic β cells, incretins are also produced and act in the CNS. GLP-1 is predominantly produced in the brainstem, from where it is transported throughout the brain to elicit metabolic, vascular, and neuroprotective actions. Peripheral GLP-1 produced by the L-cells can also communicate with the brain by crossing the BBB, or via sensory afferent vagal neurons. GLP-1R is also expressed throughout the brain, in regions that control glucose homeostasis, gut motility, food intake,

aversive signalling, cardiovascular function, and furthermore it exerts neuroprotective and neurotrophic effects, with possible implications for the treatment of neurodegenerative diseases. However, whether GLP-1 elicits direct neuroprotective/neuroregenerative effects or acts in the brain through indirect mechanisms is still unclear (Harkavyi & Whitton, 2010).

GIP production in the CNS has also been described; GIPR is expressed in the hippocampus, hypothalamus, thalamus, cerebellum, cerebral cortex, and olfactory bulb in rats and in the hippocampus and neocortex of human individuals. Whether GIP crosses the BBB in physiologically relevant concentrations is not clear; hence, the relative importance of central versus peripheral-derived GIP remains uncertain (Campbell & Drucker, 2013).

GLP-1R is a member of a different classes of receptors compared with the insulin receptor. Activation of the GLP-1R activates an adenylyl cyclase and increases cAMP levels. Thus activating PKA and other downstream kinases that are related to growth factor signalling. Although these mechanisms are not yet fully understood, they may be the reason why GLP-1 mimetics can compensate for insulin desensitisation in diabetes and in Alzheimer's disease (AD) models (Figure 9).

Despite some clear differences between the most common neurodegenerative disorders, including MS, Parkinson's disease (PD) and AD, they share several mechanisms and pathological features, e.g. apoptosis, chronic inflammatory response with associated production of cytokines and free radicals, reduced neurogenesis, synaptic failure and loss, and neuronal death. Despite the exact processes that lead to each disease are not yet fully understood, several risk factors that increase the likelihood to develop these diseases have already been identified, being T2DM one of them. This indicates that insulin desensitisation in the periphery may be a factor in inducting or rushing the development of neurodegenerative processes (Hölscher, 2012, 2014). Several epidemiological studies found a correlation between T2DM and an increased risk of developing certain neurodegenerative diseases such as AD (Luchsinger *et al.*, 2004; Haan, 2006) and PD (Aviles-Olmos *et al.*, 2013; Lijun *et al.*, 2016) at a latter state in life.

Biochemical studies of brain tissue demonstrate that insulin receptors and signalling are desensitised and impaired in AD patients, drawing attention to possible shared pathways with T2DM that can be relevant, in pathophysiological terms, and in approaching common therapeutic strategies.

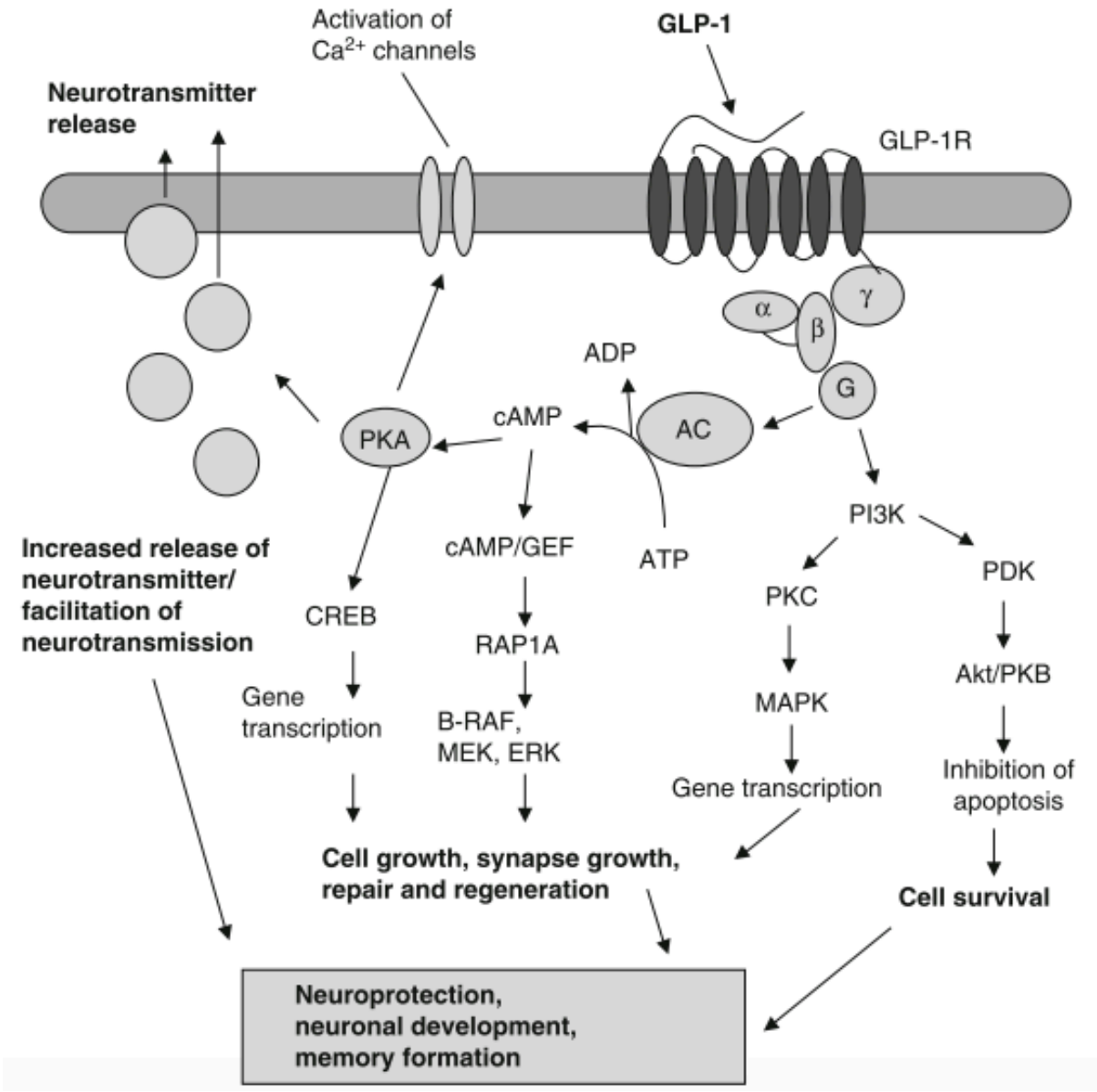

Figure 9. Activity of GLP-1 in neurons. Activation of the GLP-1R activates an adenylyl cyclase and increases cAMP levels. This activates PKA and other downstream kinases that are related to growth factor signalling. AC = andenylate cyclase; ADP = adenosine diphosphate; ATP = adenosine triphosphate; cAMP = cyclic adenosine monophosphate; CREB = cAMP response element-binding; ERK = extracellular signal-regulated kinase; G = guanine nucleotide-binding protein; GEF = guanosine exchange factor; GLP-1 = glucagon-like peptide-1; GLP-1R = glucagon-like peptide-1 receptor; MAPK = mitogen-activated protein kinase; PDK = pyruvate dehydrogenase kinase; PI3K = phosphatidylinositol 3-kinase; PKA = protein kinase A; PKB = protein kinase B; PKC = protein kinase C (taken from Hölscher, 2014).

3.4. Multiple sclerosis

Since GLP-1 has anti-inflammatory properties, as well as ability to protect synapses from stressors, DPP-IV inhibitors may have beneficial effects in the treatment of MS.

At present, there are no scientific reports on the effects of GLP-1 mimetics in animal models of MS. However, a patent that reports the effects of exendin-4[6] in mouse models of MS is available ('GLP-1R agonists for treating autoimmune disorders' [WO 2011/024110A2] by the companies Pfizer and Rinat Neuroscience Corporation). This patent intends to report the effects of exedin-4 and GLP-1 in several MS mouse models (e.g. EAE). According to the patent, spinal cord sections were analysed for infiltrating cells, T cells, monocytes and microglia. Levels of demyelination were also assessed, such as cytokine expression, e.g. interleukin-17 (IL-17) and interferon-γ. Animals' motor activity was also scored, and survival times were quantified. After treatment with exendin-4, mice's motor impairment showed a reduction and life expectancy was increased. The drug also reduced the inflammatory response, such as T-cell activation and proliferation, among the inflammatory cell invasion into the CNS. Activation of microglia and macrophages also declined, as well as cytokine production in the spleen and demyelination levels (Chou *et al.*, 2011).

These preclinical results are promising and encouraging and may indicate that GLP-1 has beneficial effects in patients with MS, and GLP-1R agonists (as well as DPP-IV inhibitors) may also be helpful in the treatment of these patients (Yazbeck *et al.*, 2009; Harkavyi & Whitton, 2010; Kim *et al.*, 2014).

Furthermore, T-cell clones from MS patients have shown to express significantly higher DPP-IV levels. Likewise, DPP-IV inhibitors have been recently studied in blood samples from patients with MS and in EAE animal model. Those drugs inhibited production of IL-4, IFN-γ, and TNF-α, suggesting that DPP-IV inhibitors may suppress the inflammatory response associated with MS (Steinbrecher *et al.*, 2001; Biton *et al.*, 2006; Yazbeck *et al.*, 2009; Kim *et al.*, 2014).

[6] A 39 amino acid peptide isolated from the saliva or venom of the lizard *Heloderma suspectum*, native to the southern desert regions of the USA. It shows an almost identical pharmacodynamic profile to GLP-1, it's also a GLP-1R agonist, but has a substantially longer plasma half-life since it is not metabolized by DPP-IV, which metabolizes GLP-1 rapidly

Chapter 4
Objectives

The main aim of this study was to characterize behaviour and biochemical profiles associated with demyelination and spontaneous remyelination in an animal model of MS induced by CPZ intoxication, using the corpus callosum and the cerebellum as target brain regions. In order to accomplish that, this experimental animal model was characterized at the peak of demyelination (after 5 weeks of CPZ ingestion, W5), and at an early stage of spontaneous remyelination (two weeks after CPZ removal, W7).

In particular, the following specific aims were pursuit:

- evaluate the existence of behaviour changes;
- access the expression of markers of neurotoxicity (glial fibrillary acidic protein, GFAP, specific main constituent of intermediate filaments in astrocytes) and demyelination (myelin-PLP, one of the main myelin protein from the CNS, which plays an important role in the formation or maintenance of the multilamellar structure of myelin);
- quantify the expression of inflammatory mediators (IL-1β, and TNF-α);
- estimate the expression of DPP-IV, GLP-1 and GLP-1R in the target brain areas.

PART II

EXPERIMENTS AND ACHIEVEMENTS

Chapter 5
Materials and methods

5.1 Animals and treatments

A total of 40 C57BL/6 male mice (Charles River Laboratories, Barcelona, Spain) were used; animals were housed two or four per cage in the experimental vivarium of the Laboratory Pharmacology and Experimental Therapeutics at the IBILI, Faculty of Medicine, University of Coimbra, under controlled temperature (22 ± 1 ºC), humidity (50 ± 10 %) and lighting (12:12 h light-dark cycle). On the arrival, mice with 6 weeks were given standard chow (containing 16.1% protein, 3.1% lipids, 3.9% fibbers and 5.1% minerals – AO4 Panlab, Barcelona, Spain) and water *ad libitum*.

After 2 weeks of acclimatization, animals were randomly divided into two groups: the control (Ctrl) group, a total of 20 mice, which continued to receive tap water for drinking; and the CPZ group, another 20 mice which received tap water mixed with 0.2% (w/v) CPZ (*C9012* Sigma-Aldrich, Sintra, Portugal). All animals were fed standard mice chow.

After 5 weeks of exposure to CPZ (13 weeks of age), half of the animals (from both Ctrl and CPZ, W5 groups) were submitted to behavioural tests and subsequently sacrificed. The other half remained under study for another 2 weeks. At this stage, CPZ was removed from the diet in order to allow spontaneous remyelination of the CNS in the CPZ group. At the end of that period (15 weeks of age) all the mice (Ctrl and CPZ, W7) were submitted to the same behavioural testes and then sacrificed.

Each animal's body weight was evaluated at the beginning of experiments (beginning of CPZ administration), after 5 weeks of CPZ administration, as well as after 2 weeks of CPZ

withdrawal (7 weeks). Measures were conducted with an analytical balance (KERN CB 6 K1, Germany).

All experiments were conducted according to the European Community Council Directive on Animal Care 2010/63/EU, transposed to Portuguese law in Decreto Lei nº 113/2013.

5.2 Behavioural testing

Animal behavioural experiments were conducted in order to identify differences between Ctrl and CPZ-fed mice at the peak of demyelination (5 weeks of CPZ administration, W5) and at a phase of early remyelination (2 weeks after CPZ suspension, W7). Animals were subjected to behavioural experiments that evaluated spontaneous exploration (open field and Y-maze), anxiety-related behaviour (open field and splash test) and motor activity (open-field).

All tests were performed avoiding human contact with animals, in order not to bias the results of the experiments. Therefore, all tests were recorded by a video camera on the ceiling of the room for filming the entire apparel (Wahlsten, 2011). Results were analysed with the behaviour tracking software ANY-maze.

5.2.1 Symmetrical Y maze test

The Y maze test is a simple recognition test for measuring short-term spatial working memory. The apparel is a maze with three identical arms (25 cm each), which evoke active exploration. Each mouse is placed at the end of one arm and allowed to move freely through the maze (Figure 10) for an 8 min test period.

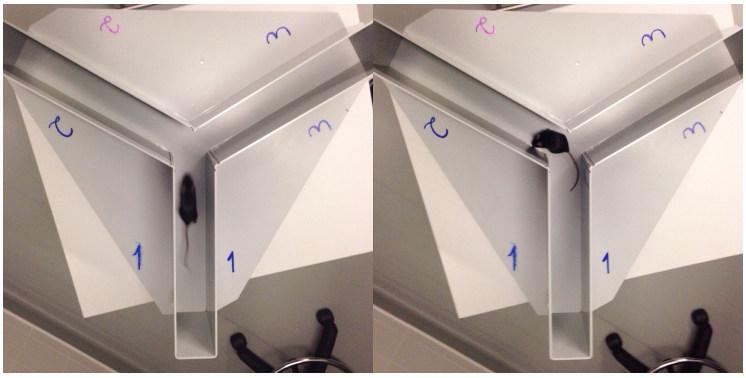

Figure 10. Representative images of Y Maze test. Mice was placed in arm 1, and then allowed to walk freely in the maze.

The number of arm entries, as well as the pattern of entries, must be identified in order to calculate the number of alternations. The mouse must return to the hub of the maze after each arm entry, and it can then return to the arm it just visited, the arm it visited on the previous entry, or the one least recently visited. An alternation is defined as successive entries into the three arms on the overlapping triplet set, which means that in order to do an alternation the mouse must enter the least recently visited arm. When the animal goes to the most recently visited arm it's called a prior entry. Subsequently, the spontaneous alternation behaviour (SAB) is determined:

$$SAB = \frac{number\ of\ alternations}{total\ number\ of\ entries - 2}$$

The short-term working memory interpretation of alternation asserts that preference for the least visited arm indicates memory for the history of arm entries (Wahlsten, 2011).

5.2.2 Square open field test

A featureless square box (45×45 cm and 45 cm of high) barren of all structures yields a convenient index of the tendency to move in an environment (Figure 11). At the beginning of the test, the mouse is placed alone at the centre of the box, and is allowed to move freely during the 15 minutes of the test. Overall activity level is monitorized by video and posteriorly evaluated, measuring the total length of the path travelled by the mouse. Some mice tend to hug the walls, avoiding the centre of the chamber, which is an indicator of anxiety-related

behaviour; this exploratory activity was measured by the length in the central area of the path travelled by the mouse. The central area corresponds to the internal section that distance 10 cm of each wall. Behaviours such as leaning against a wall or rearing when away from a wall, are correlated with activity levels, and those were also counted (Wahlsten, 2011).

Figure 11. Representative images of the open field test. Mice is placed in the centre of the maze and allowed to explore the apparel**.**

5.2.3 Splash test

The splash test consists in the application of 10% (w/v) sucrose (Sigma-Aldrich, Sintra, Portugal) on the back of the mouse with a wash bottle (Figure 12). Since this solution is viscous, the animal's fur will be smutty, so the animal will have to lick it to become clean. This test is performed in an opaque box, so animals can't see each other being tested. First animals spent a 2 minutes period in the box so they can adapt to the new environment; subsequently, sucrose solution is added and the time spent cleaning the fur is measured, in a total of 5 minutes. The time spent taking care of the fur is related with the preservation of self-care and motivation. So, the decrease of the previous behaviour is a sign of depressive symptomatology (Wahlsten, 2011).

Figure 12. Representative image of the splash test. Image shows user applying sucrose solution on animal's back.

5.3 Animals' sacrifices and samples' collection

Two days after performing the behaviour testes, mice were subjected to intraperitoneal anaesthesia with a 2 mg/kg BW of a 50 mg/kg pentobarbital (Sigma-Aldrich, Sintra, Portugal) solution, and then sacrificed by decapitation. Brains were promptly removed and dissected on ice. Right hemisphere (sagittal section) was isolated and placed in paraformaldehyde (PFA) for posterior immunohistochemistry (IHC) analysis; furthermore, cerebellums were frozen in liquid nitrogen and stored at -80 ºC for western blot (WB) and reverse transcription polymerase chain reaction (RT-PCR) studies.

5.4 Protein expression analysis

5.4.1 Western blotting

Western blotting (WB) is an important procedure for the immunodetection of specific proteins in a complex mixture of proteins extracted from cells. This technique involves, besides the sample preparation, separation by molecular weight, transfer of protein patterns from gel to microporous membrane, and finally marking target protein using a proper primary and secondary antibody to visualize (Kurien & Scofield, 2015).

Firstly, cerebellum extracts from the left hemisphere were homogenized in 400 µL of RIPA lysis and extraction buffer (150 mM sodium chloride [NaCl, 31434, Sigma-Aldrich]; 50 mM Tris-HCl pH=8.0 [648310, Calbiochem]; 5 mM ethylene glycol-bis[β-aminoethyl ether]-N,N,N',N'-tetraacetic acid [EGTA, E4378, Sigma-Aldrich]; 1% Triton X-100 [108643, Merk Millipore]; 0.5% [w/v] sodium deoxycholate [DOC, D6750, Sigma-Aldrich]; 0.1% sodium dodecyl sulphate [SDS, 0227, Amresco]), supplemented with protease and phosphatase inhibitor cocktail (1 mM phenylmethanesulfonyl fluoride [PMSF], 1 mM dithiothreitol [DTT], 1 µg/mL chymostatin, 1 µg/mL leupeptin, 1 µg/mL antipain, 5 µg/mL pepstatin A, 50 mM sodium fluoride and 1 mM sodium orthovanadate; Sigma-Aldrich, Sintra, Portugal). Each sample was homogenised three times with 10 sec ultrasounds pulse, and immersed in ice between each pulse, avoiding overheating of the biological material. Subsequently, the homogenates were centrifuged with 13,000 rpm (15,493 × g), for 15 min at 4ºC. The resulting

supernatant fraction (corresponding to total extract) was collected and total protein concentration was determined using the bicinchoninic assid assay (BCA, Thermoscientific), and supernatants were stored at -80ºC until further use. Thereafter, samples were denatured at 95 ºC for 5 min in sample buffer (0.5 M Tris-HCl pH=6.8, 10% [w/v] SDS, 30% [v/v] glycerol, 0.6 M DTT, 0.01% [w/v] bromophenol blue), for 6 repetitions.

For immunodetection analysis, 10 to 80 μg of protein were loaded per lane and separated by 10% or 15% SDS polyacrylamide gel electrophoresis (the first 20 min at 80 V to pass the stacking gel, and then 120 V for about an 1 hour), in running buffer, at room temperature (Laemmli U., 1970). Then, proteins were electroblotted (120 V, 90 min.) onto a polyvinylidene difluoride (PVDF) membrane (Immobilon PVDF transfer membranes 0.2 μm, Millipore, Madrid, Spain) in a transfer buffer (100 mM 3-[cyclohexylamino]-1-propanesulfonic acid [CAPS, C2632 Sigma-Aldrich], 20% [v/v] methanol [MeOH, 1060092511 Merck Millipore], pH 11). Membranes were previously activated in MeOH.

Subsequently, PVDF membranes were blocked in 5% (w/v) skim milk powder (or 1% [w/v] BSA [A9647, Sigma-Aldrich]) in phosphate buffer saline (PBS: 0.137 M NaCl, 2.7 mM potassium chloride [KCl, 529552, Calbiochem], 1.8 mM potassium phosphate [KH_2PO_4 529568, Calbiochem], 10 mM sodium dihydrogen phosphate dihydrate [$NaH_2PO_4.2H_2O$, 1063421000 Merck Millipore], pH 8.3) containing 0.1% (v/v) Tween-20 (P1379 Sigma-Aldrich) (PBS-T) for 1 hour at room temperature. Membranes were then incubated with primary antibody raised against GFAP (1:2000, mouse monoclonal antibody, IF03L Merck Millipore), myelin-PLP (1:1000, rabbit polyclonal antibody, ab28486 Abcam), TNF-α (1:100, rabbit polyclonal antibody, ab6671 Abcam), DPP-IV (1:2500, rabbit polyclonal antibody, ab28340 Abcam) and GLP-1R (1:1000, rabbit polyclonal antibody, AGR-021 Alomone) overnight at 4ºC (Table 1).

Afterwards, they were extensively washed (3–6 x 10 min) in PBS-T, with agitation, and incubated for one hour at room temperature with adequate alkaline phosphatase conjugated secondary antibodies prepared in 5 % (w/v) skim milk powder (or 1% BSA) in PBS-T. After secondary antibody incubation, membranes were once again washed for 30 min in PBS-T. To confirm equal protein loading and sample, transfer blots were reprobed with either mouse anti-β-actin or mouse anti-(glyceraldehyde 3-phosphate dehydrogenase) (GAPDH).

After reacting with enhanced chemifluorescence detection reagent (ECF, Enhanced Chemifluorescence – GE Healthcare), immunoreactive bands were revealed by scanning blots using a Fluorescent image analyser Typhoon FLA 900 (GE Healthcare Bio-Sciences) imaging system. Densitometric analyses were performed using the Image Quant 5.0 software (Molecular

Dynamics). Results were normalized against β-actin or GAPDH and then expressed as percentage of control (Kurien & Scofield, 2015).

Table 1. List of primary and secondary antibodies used for WB analysis

Antibody	Molecular Weight (kDa)	Loading (µg)	Dilution	Acrylamide Gel (%)	Reference
Mouse Monoclonal Anti-GFAP	50	10	1:2000	10	IF03L Merk Millipore
Rabbit Polyclonal Anti-PLP	26.30	40	1:1000	15	ab28486 Abcam
Rabbit Polyclonal TNF-α	17	80	1:1000	15	ab6671 Abcam
Rabbit Polyclonal Anti-GLP-1R	100-130	40	1:1000	10	AGR-021 Alomone
Rabbit Polyclonal Anti-DPP-IV	88	80	1:2500	10	ab28340 Abcam
Mouse Anti-β-Actin	42	–	1:5000	–	a5316 Sigma-Aldrich
Mouse Anti-GAPDH	38	–	1:5000	–	MAB374 Millipore
Goat Anti-Mouse	–	–	1:5000	–	B3582 Sigma-Aldrich
Goat Anti-Rabbit	–	–	1:5000	–	NIF1317 GF Healthcare

5.4.2 Immunohistochemistry

Right hemisphere samples were fixed with 4% PFA during 24 hours, and then transposed to a 20% sucrose solution. Following 2 days, sucrose solution was removed and tissues were embed in optimal cutting temperature (OCT) compound and frozen, at -80ºC, until further use.

For IHC analysis, slices (30 µM) from right hemisphere, containing cerebellum and corpus callosum, were obtained in a cryostat (Leica CM3050 S, Wetzlar, Germany) and immediately placed in PBS solution. Subsequently, samples were washed twice with PBS under agitation, and then fixed with a solution of 4% PFA and 4% sucrose for 1 hour at room temperature and subsequently rinsed again with PBS three times. To prevent unspecific

binding, tissues were permeabilized with 300 µL blocking solution (1% BSA, 1% Triton X-100 in PBS). After blocking for 2 hours, slices were incubated with the primary antibodies, diluted in blocking solution. Following 48 hours of incubation, slices were rinsed three times with PBS under agitation, and afterwards incubated on dark with secondary antibody, also diluted in blocking solution and 4',6-diamidino-2-phenylindole (DAPI, 1:2000) to stain the nuclei (Table 2). After washing three times in PBS, the coverslips were mounted on glass slides using Glycergel™ mounting medium (Dako, Agilent Technologies, Santa Clara, CA, USA). Images were acquired in a laser scanning confocal microscope LSM 710 (Zeiss, Oberkochen, Germany). For a negative experiment, the primary antibody was omitted (Buchwalow & Böcker, 2010; Lin & Prichard, 2015).

Table 2. List of primary and secondary antibodies used for IHC analysis

Antibody	Dilution	Reference
Rabbit Polyclonal Anti-PLP	1:100	ab28486 Abcam
Mouse Monoclonal Anti-GFAP	1:500	IF03L Merck Millipore
Rabbit Polyclonal Anti-DPP-IV	1:100	ab28340 Abcam
Rabbit Polyclonal Anti-GLP-1R	1:100	AGR-021 Alomone
AF 568 Goat Anti-Rabbit	1:500	A-11011 Molecular Probes
AF 488 Goat Anti-Rabbit	1:500	A-11008 Molecular Probes
AF 568 Goat Anti-Mouse	1:500	A-11004 Molecular Probes

5.5 Gene expression analysis

Total RNA was isolated from cerebellum and corpus callosum using TRIzol™ reagent (Ambion, Life Technologies, Grand Island, NY, USA). Subsequently, cDNA first strand synthesis was performed from 2 μg DNase-treated RNA using random primers and SuperScript II Reverse Transcriptase (Invitrogen, Life Technologies). The resulting cDNA (0.5 μL) was used for amplification of respective targets with AmpliTaq Gold DNA polymerase (Applied Biosystems, Life Technologies), 200 nM of primer and 2 mM $MgCl_2$, in a Veriti thermal cycler (Applied Biosystems). Cycling conditions were a melting step at 95°C for 15 sec, annealing elongation at 60ºC for 45 sec, and extension at 72ºC, with 40 cycles. Used primers are indicated in Table 3. PCR products were separated on a 1.5% agarose gel. β-actin was used as an internal control. Gel images were digitally acquired in a Gel/ChemiDoc (Bio-Rad Laboratories, Hercules, CA, USA) and the level of gene transcription was evaluated and categorized as detected or not detected.

Table 3: List of primers' sequences for RT-PCR

Gene	Primer Sequence	Annealing Temperature
PLP	Forward: 5' – CAGGCAGATCTTTGGCGACT – 3' Reverse: 5' – GTGATGCCCACAAACGTTGC – 3'	60 ºC
IL-1β	Forward: 5' – GGACAGAATATCAACCAACA – 3' Reverse: 5' – ACACAGGACAGGTATAGATT – 3'	60 ºC
TNF-α	Forward: 5' – ATGGCCTCCCTCTCATCAGT – 3' Reverse: 5' – TGGTTTGCTACGACGTGGG – 3'	60 ºC
DPP-IV	Forward: 5' – CAAGCAATGTGGTACACGGAT – 3' Reverse: 5' – GAGGAAATGGCTCATGTGGGA – 3'	60 ºC
GLP-1	Forward: 5' – CCAAGATCACTGACAAGAAATAGGT – 3' Reverse: 5' – TGTACATCCCAAGTGACTGGC – 3'	58 ºC
GLP-1R	Forward: 5' – AGTTCCGCTGCTGTTCGTTA – 3' Reverse: 5' – TTCCTAGTCCAGCAGCCCTC – 3'	60 ºC

5.6 Statistical analysis

Results were expressed as means ± standard errors of the mean (SEM) and percentage of the control, as indicated. Comparisons between groups were analysed by one-way analysis of variance (ANOVA) test, corrected for multiple comparisons using the Bonferroni's statistical hypothesis test. When appropriate a student's t-test was used. Differences were considered to be significant at $p<0.05$ (*/#), $p<0.01$ (**/##) and $p<0.001$ (***/###). Symbol * refers to comparisons between Ctrl groups, and # between CPZ groups.

Statistical analysis was obtained using GraphPad Prism software, Version 7.0 software for OS X.

Chapter 6
Results

6.1 Behavioural tests

Besides the following presented results, video footages showed clear motor impairment of mice after 5 weeks of CPZ-intoxication, when compared with the control animals.

6.1.1 Y-maze test

The animals' performance on the Y-maze test was accessed by quantifying the spontaneous alternation behaviour (SAB), previously defined in the methods section. No differences were observed between the control and the CPZ-treated mice at week 5 (W5), as well as after suspension of CPZ treatment (week 7, W7) (Figure 13).

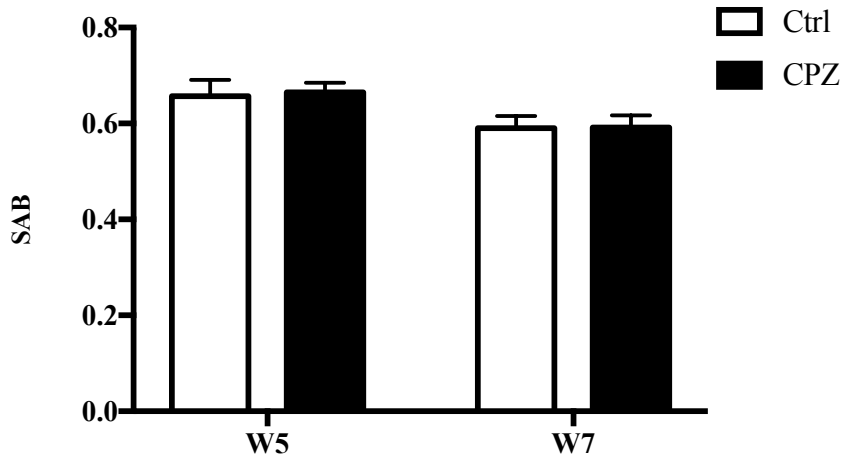

Figure 13. Y-maze performance, evaluated as SAB, in the control and CPZ-treated mice at week 5 (demyelination) and week 7 (remyelination). Results expressed in ratio between performed alternations with total possible alternations. Results presented as means ± SEM. n=10 for each group.

6.1.2 Open field test

The open field test allows the analysis of different parameters. No differences were found between groups in travelled distance and time spent on central area, and neither on time inactive (Figure 14 A, B and C). Nevertheless, demyelinated animals (CPZ W5) tended to perform less rearings than control ones (Figure 14 D and E).

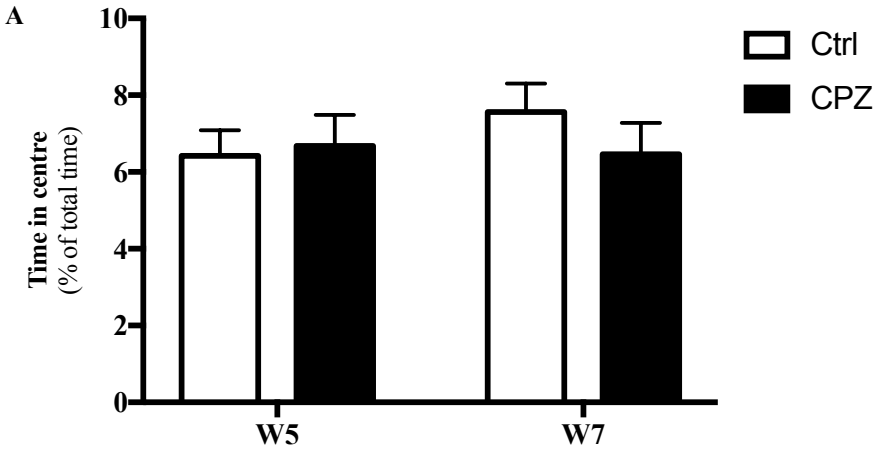

B

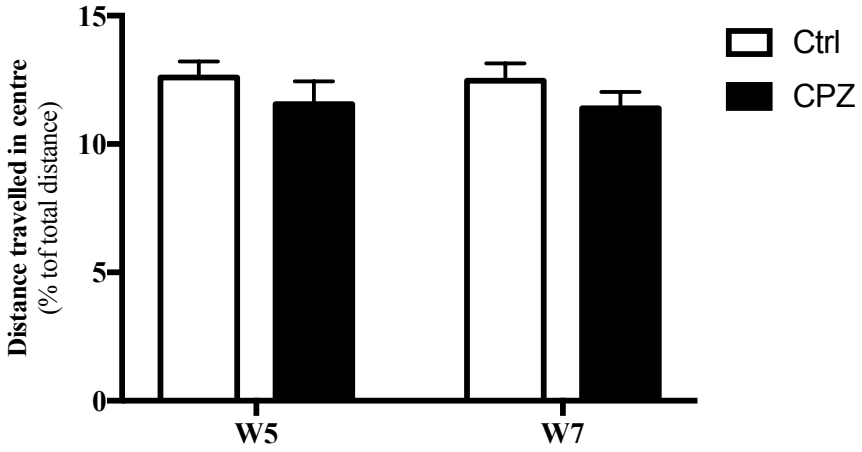
Distance travelled in centre
(% tof total distance)
15
10
5
0
W5
W7
Ctrl
CPZ

C

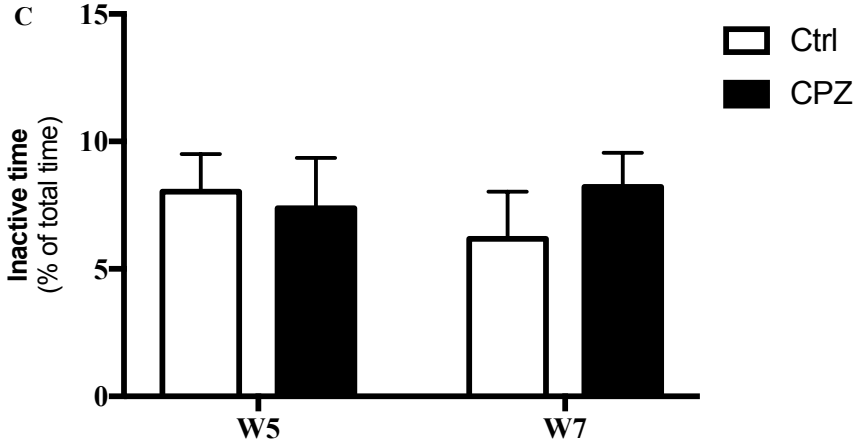
Inactive time
(% of total time)
15
10
5
0
W5
W7
Ctrl
CPZ

D

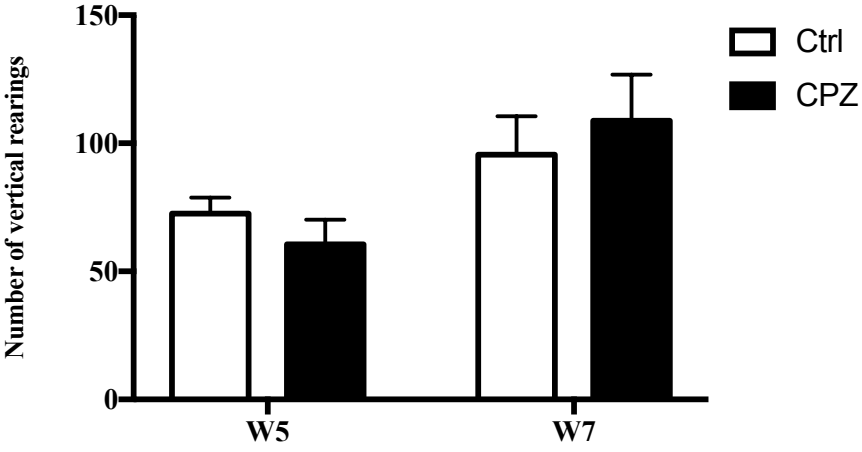
Number of vertical rearings
150
100
50
0
W5
W7
Ctrl
CPZ

E

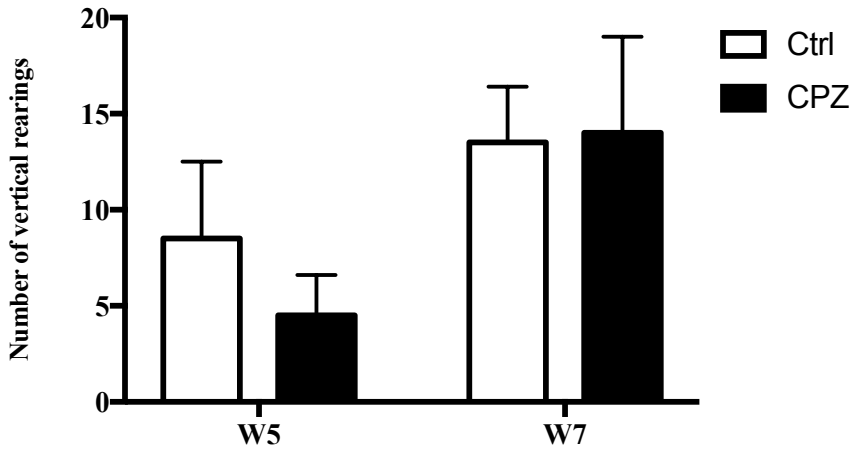

Figure 14. Open field test results in the control and CPZ-treated mice at week 5 (demyelination) and week 7 (remyelination). (A) Time mice spent on central area. Results are expressed as percentage of total time of experiment and presented as means ± SEM. n=10 for each group. (B) Mice's travelled distance on central area. Results are expressed as percentage of total travelled distance and presented as means ± SEM. n=10 for each group. (C) Time spent inactive. Results are expressed as percentage of total time of experiment and presented as means ± SEM. n=10 for each group. (D) Number of total performed rearings. Results presented as means ± SEM. n=4 for each group (E) Number of performed central rearings. Results presented as means ± SEM. n=4 for each group.

6.1.3 Splash test

After 5 weeks of CPZ intoxication (W5 CPZ), the time CPZ-treated mice spent taking care of their fur (grooming time) tended to decrease when compared with that of the Ctrl animals. However, CPZ-treated mice tended to become more self-care after 2 weeks of CPZ withdrawal (W7 CPZ), returning to values identical to those of the control group (Figure 15).

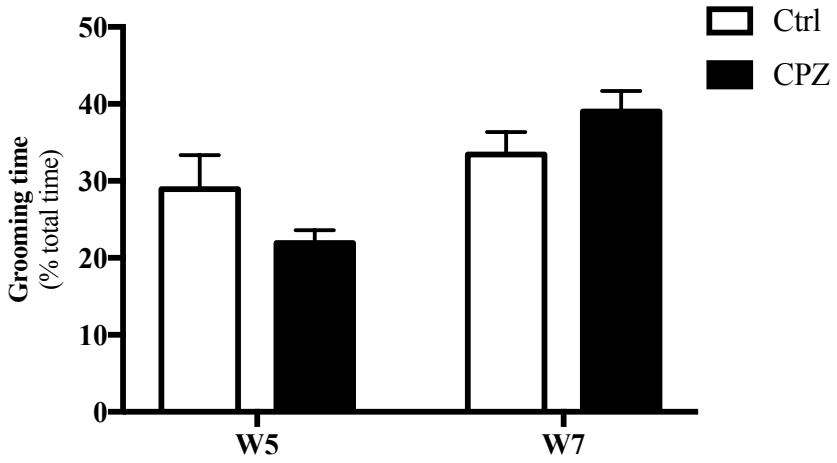

Figure 15. Splash test results (time spend on grooming) in the control and CPZ-treated mice at week 5 (demyelination) and week 7 (remyelination). Results are expressed as percentage of test time and presented as means ± SEM. n=10 for each group.

6.2 Proteins and genes' expression

6.2.1 GFAP expression

In the cerebellum, after 5 weeks of CPZ intoxication, there was a significantly increased GFAP protein expression in the cerebellum in the CPZ-treated versus untreated (Ctrl) mice (154.21 ± 19.03 % *vs* 100.00 ± 14.30 %; *p<0.05). The effect was then abolished after 2 weeks of CPZ withdrawal, approaching the Ctrl levels. The reduction observed between weeks 5 and 7 in the CPZ-treated animals was statistically significant (154.21 ± 19.03 % *vs* 96.78 ± 7.08 %, #p<0.05) (Figure 16).

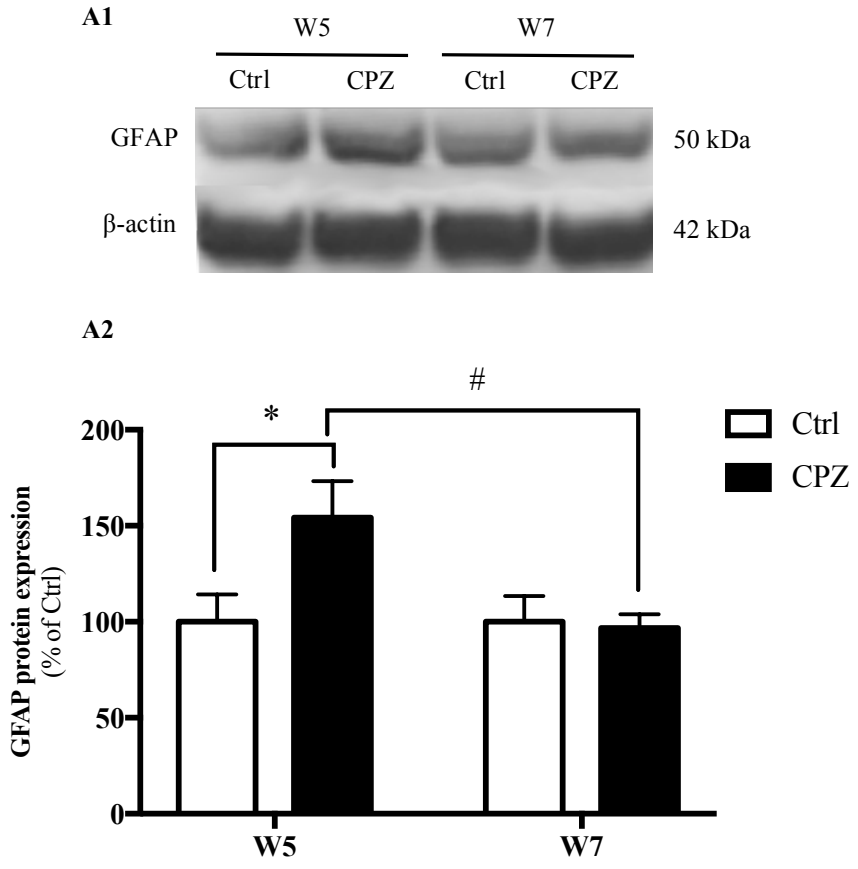

Figure 16. GFAP protein expression in the cerebellum at peak of demyelination (W5) and early remyelination (W7). (A1) Representative WB bands of GFAP expression. β-actin was used as the internal control. (A2) Quantification of GFAP protein expression after CPZ-intoxication (W5) and toxin withdrawal (W7), compared with a control for each group (Ctrl W5 and Ctrl W7). Results are expressed as percentage of the control and presented as means ± SEM; n=7 for each group; *p<0.05 vs Ctrl, #p<0.05 vs CPZ; one-way ANOVA followed by Bonferroni's test.

In corpus callosum, IHC indicated a trend for GFAP protein content increase in demyelinated samples, when compared with control. In remyelination period, levels of GFAP seem to have decreased, to a pattern similar to control (Figure 17).

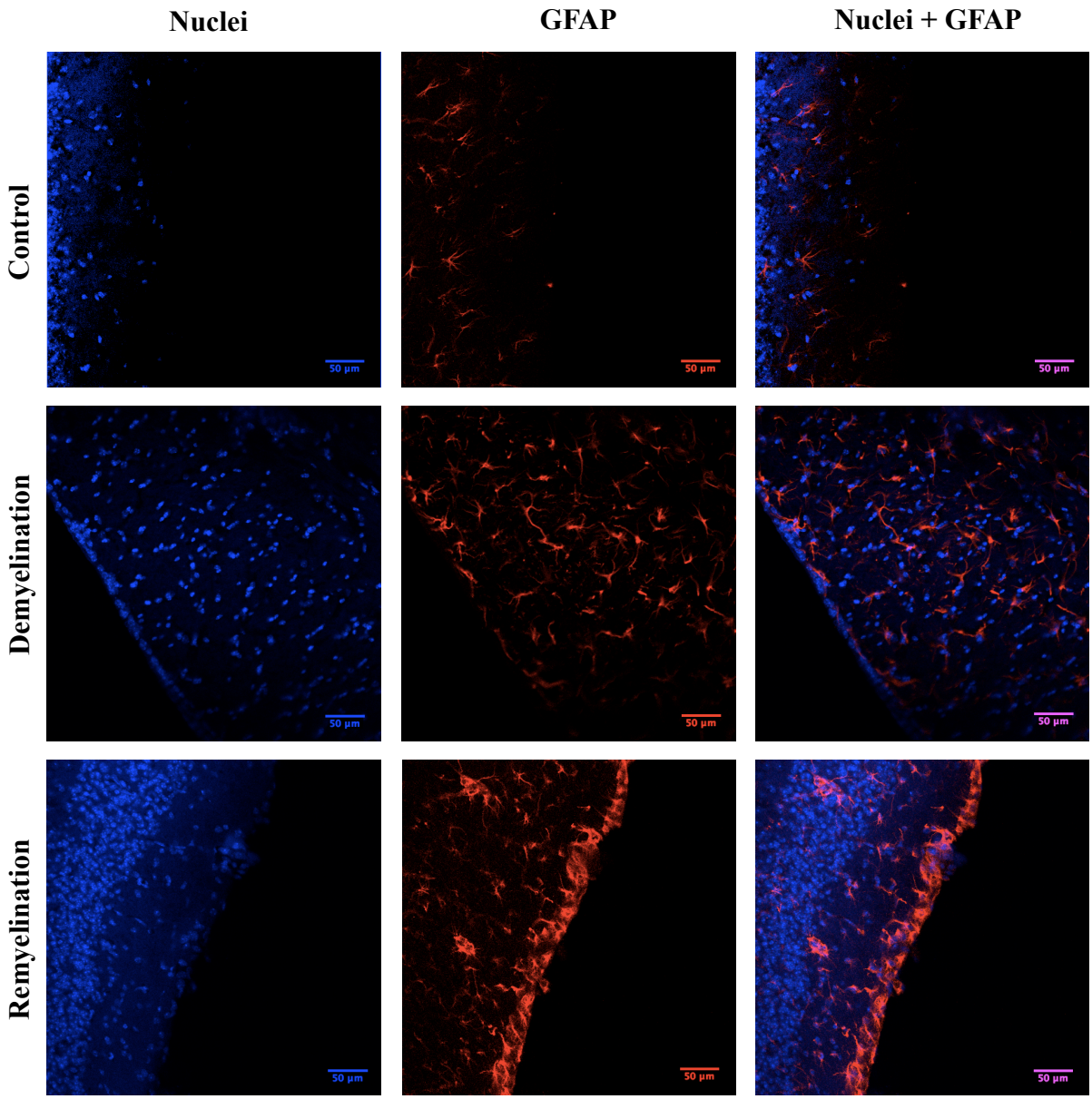

Figure 17. GFAP protein expression (immunostaining) in the corpus callosum at peak of demyelination (W5) and early-remyelination (W7). Representative images of GFAP (red) corpus callosum localization, in control, demyelination (after 5 weeks of 0.2% CPZ intoxication), and remyelination phases (after 2 weeks of CPZ-withdrawal). Nuclei are stained with DAPI (blue). Scale bar: 50 µm; n=1–2 for each group.

6.2.2 Myelin-PLP expression

In the CPZ-treated mice there was a significantly reduced myelin-PLP mRNA expression in the cerebellum after 5 weeks of CPZ treatment, when compared to the untreated (Ctrl) animals (0.45 ± 0.05 *vs* 1.01 ± 0.07, **p<0.01). After 2 weeks of CPZ withdrawal (remyelination period), the values returned to normal, approaching the Ctrl ones (Figure 18A). Identical effect, yet not statistically significant, was found for cerebellum myelin-PLP protein expression, with reduced levels at the peak of demyelination (week 5) and normalized after remyelination (week 7), when compared with the control animals (Figure 18B).

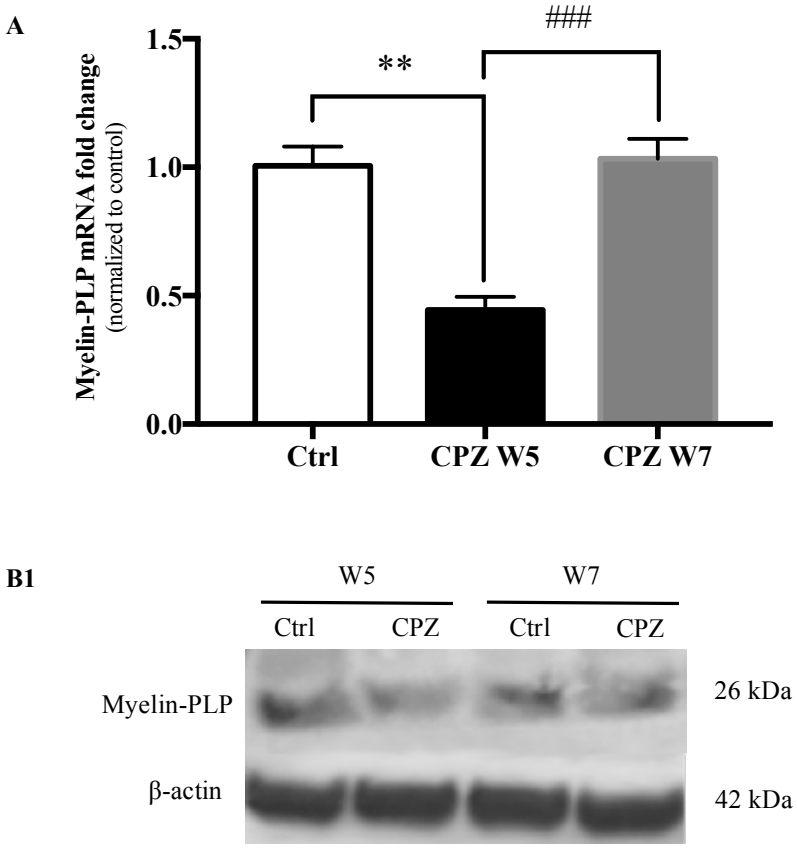

B2

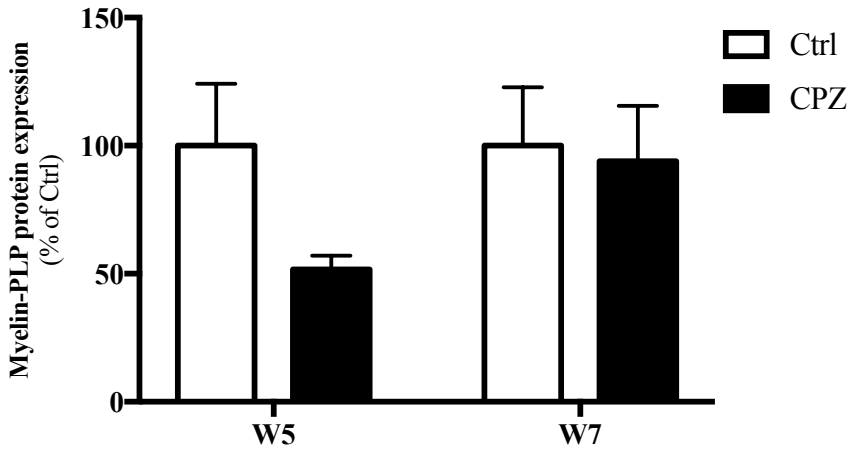

Figure 18. Myelin-PLP protein and gene expression in the cerebellum at peak of demyelination (W5) and early-remyelination (W7). (A) Quantification of myelin-PLP gene expression in control (Ctrl), CPZ-intoxication (CPZ W5) and toxin withdrawal (CPZ W7) groups. Results normalized to control and presented as means ± SEM. n=3 for Ctrl and n=4 for each CPZ group; **p<0.01 vs Ctrl, ###p<0.001 vs CPZ; one-way ANOVA followed by Bonferroni's test. (B1) Representative WB bands of myelin-PLP expression. β-actin was used as the internal control. (B2) Quantification of GFAP protein expression after CPZ-intoxication (CPZ W5) and toxin withdrawal (CPZ W7) compared with a control for each group (Ctrl W5 and Ctrl W7). Results are expressed as percentage of the control and presented as means ± SEM; n=7 for each group.

In the corpus callosum, there was a clear reduction of myelin-PLP protein immunostaining in the demyelination stage, when compared with control. In the remyelination period, myelin-PLP expression was recovered, although with an imperfect pattern, at least comparing with the control (Figure 19).

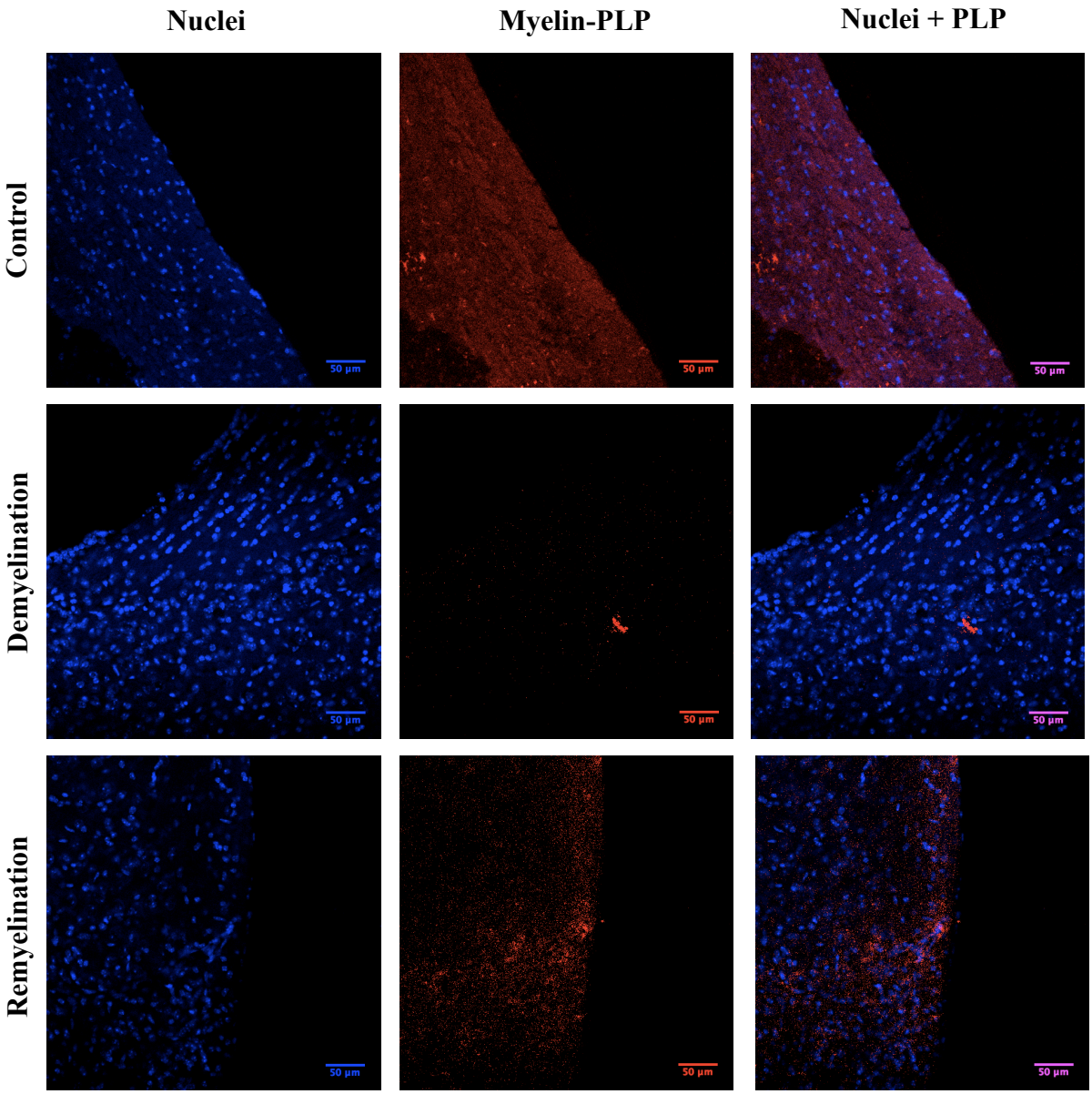

Figure 19. Myelin-PLP protein expression (immunostaining) in the corpus callosum at peak of demyelination (W5) and early-remyelination (W7). Representative images of myelin-PLP (red) corpus callosum localization, in control, demyelination (after 5 weeks of 0.2% CPZ intoxication), and remyelination phases (after 2 weeks of CPZ-withdrawal). Nuclei are stained with DAPI (blue). Scale bar: 50 µm; n=1–2 for each group.

6.2.3 IL-1β expression

In the cerebellum, 5 weeks after CPZ intoxication, there was a significantly increased IL-1β mRNA expression in the CPZ-treated mice, when compared with the Ctrl animals (2.11 ± 0.20 *vs* 1.03 ± 0.17; **p<0.01). After, 2 weeks of CPZ withdrawal, IL-1β mRNA levels approached the control ones, being significantly lower than those found at week 5 (peak of demyelination) in the CPZ-treated mice (1.08 ± 0.06 *vs* 2.11 ± 0.20; ##p<0.01) (Figure 20).

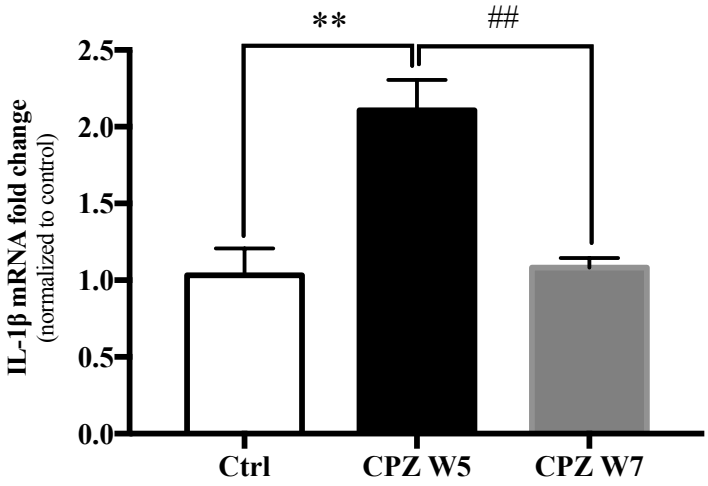

Figure 20. IL-1β mRNA expression in the cerebellum at peak of demyelination (W5) and early-remyelination (W7). Quantification of IL-1β gene expression in control (Ctrl), CPZ-intoxication (CPZ W5) and toxin withdrawal (CPZ W7) groups. Results were normalized to control and presented as means ± SEM. n=3 for Ctrl and n=4 for each CPZ group; **p<0.01 *vs* Ctrl, ##p<0.01 *vs* CPZ; one-way ANOVA followed by Bonferroni's test.

6.2.4 TNF-α expression

In the CPZ-treated mice there was a significantly higher TNF-α mRNA expression in the cerebellum, when compared with the untreated (Ctrl) animals (2.11 ± 0.20 *vs* 1.03 ± 0.17). The change was then abolished after 2 weeks of CPZ withdrawal (remyelination) (Figure 21A). This profile was identical to that found for cerebellum TNF-α protein expression, with overexpression at week 5, versus the control animals (253.20 ± 73.75 % *vs* 100.00 ± 14.28 %), then returning to basal levels at week 7 (remyelination) (Figure 21B).

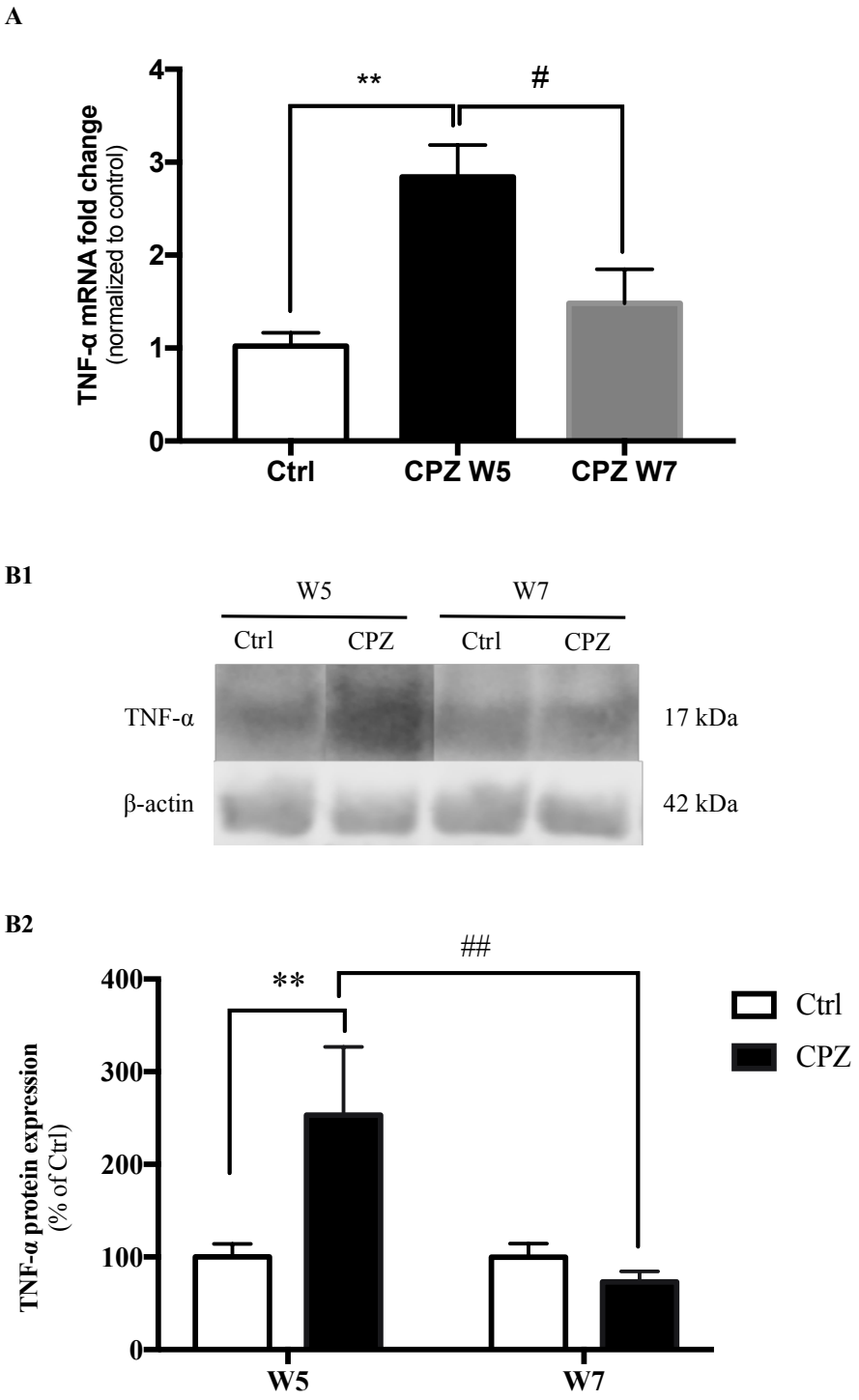

Figure 21. TNF-α protein and mRNA expression in cerebellum at peak of demyelination (W5) and early-remyelination (W7). (A) Quantification of TNF-α gene expression in control (Ctrl), CPZ-intoxication (CPZ W5) and toxin withdrawal (CPZ W7) groups. Results were normalized to control and presented as means ± SEM. n=3 for Ctrl and n=4 for each CPZ group; **p<0.01 *vs* Ctrl, #p<0.05 *vs* CPZ; one-way ANOVA followed by Bonferroni's test. (B1) Representative WB bands of TNF-α expression. β-actin was used as the internal control. (B2) Quantification of TNF-α protein expression after CPZ-intoxication (CPZ W5) and toxin withdrawal (CPZ W7) compared with a control for each group (Ctrl W5 and Ctrl W7). Results are expressed as percentage of the control and presented as means ± SEM; n=7 for each group; **p<0.01 *vs* Ctrl, ##p<0.01 *vs* CPZ; one-way ANOVA followed by Bonferroni's test.

6.2.5 DPP-IV expression

In the cerebellum, no differences in DPP-IV mRNA (Figure 22A) and protein (Figure 22B) expression were observed between the groups.

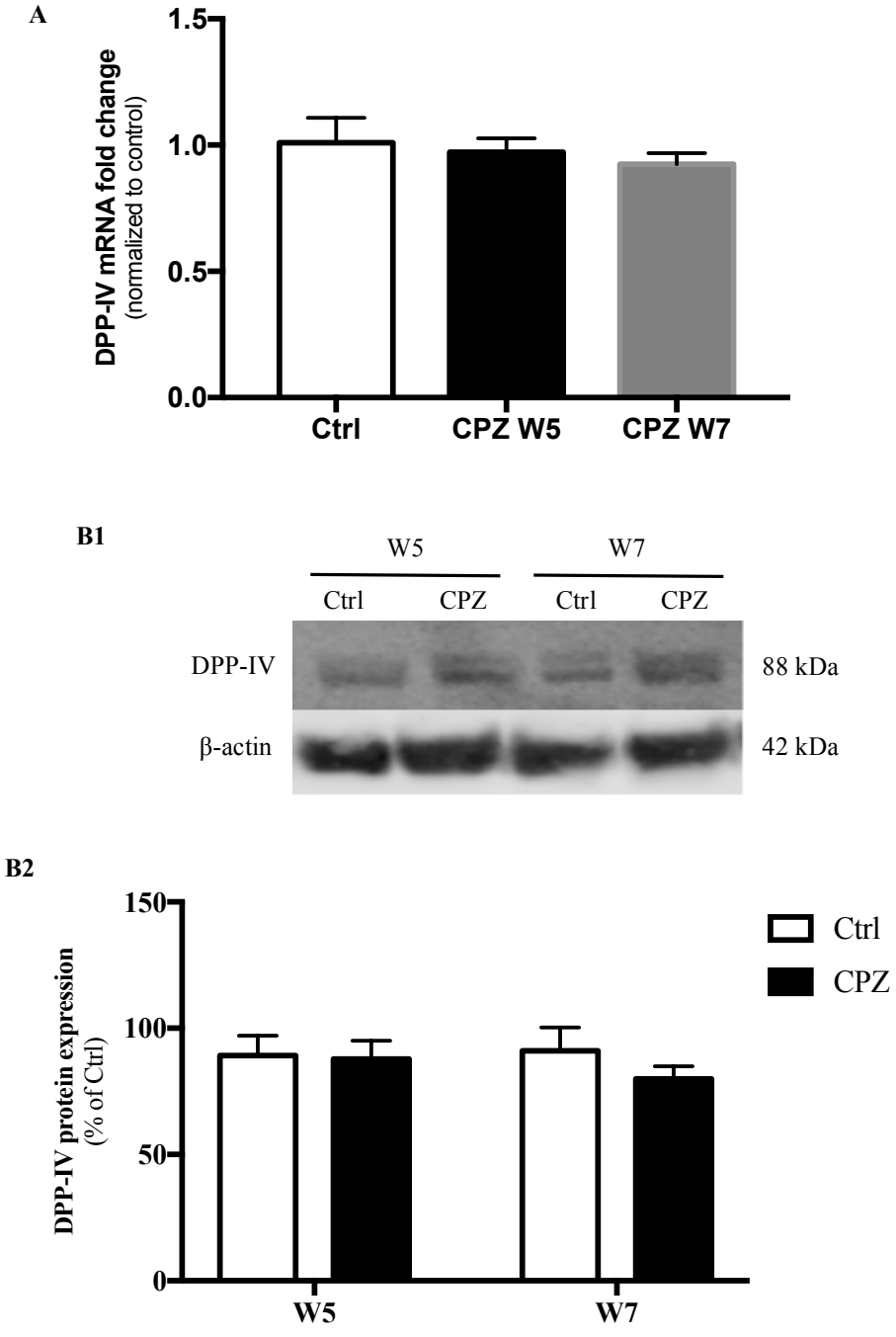

Figure 22. DPP-IV protein and gene expression in the cerebellum at peak of demyelination (W5) and early-remyelination (W7). (A) Quantification of DPP-IV gene expression in control (Ctrl), CPZ-intoxication (CPZ W5) and toxin withdrawal (CPZ W7) groups. Results were normalized to control and presented as means ± SEM. n=3 for Ctrl and n=4 for each CPZ group. (B1) Representative WB bands of DPP-IV expression. β-actin was used as the internal control. (B2) Quantification of DPP-IV protein expression after CPZ-intoxication (CPZ W5) and toxin withdrawal (CPZ W7) compared with a control for each group (Ctrl W5 and Ctrl W7). Results are expressed as percentage of the control and presented as means ± SEM; n=7 for each group.

In the corpus callosum, a trend for increased DPP-IV expression (immunostaining) was found in demyelinated samples, when compared with the control ones (Figure 23).

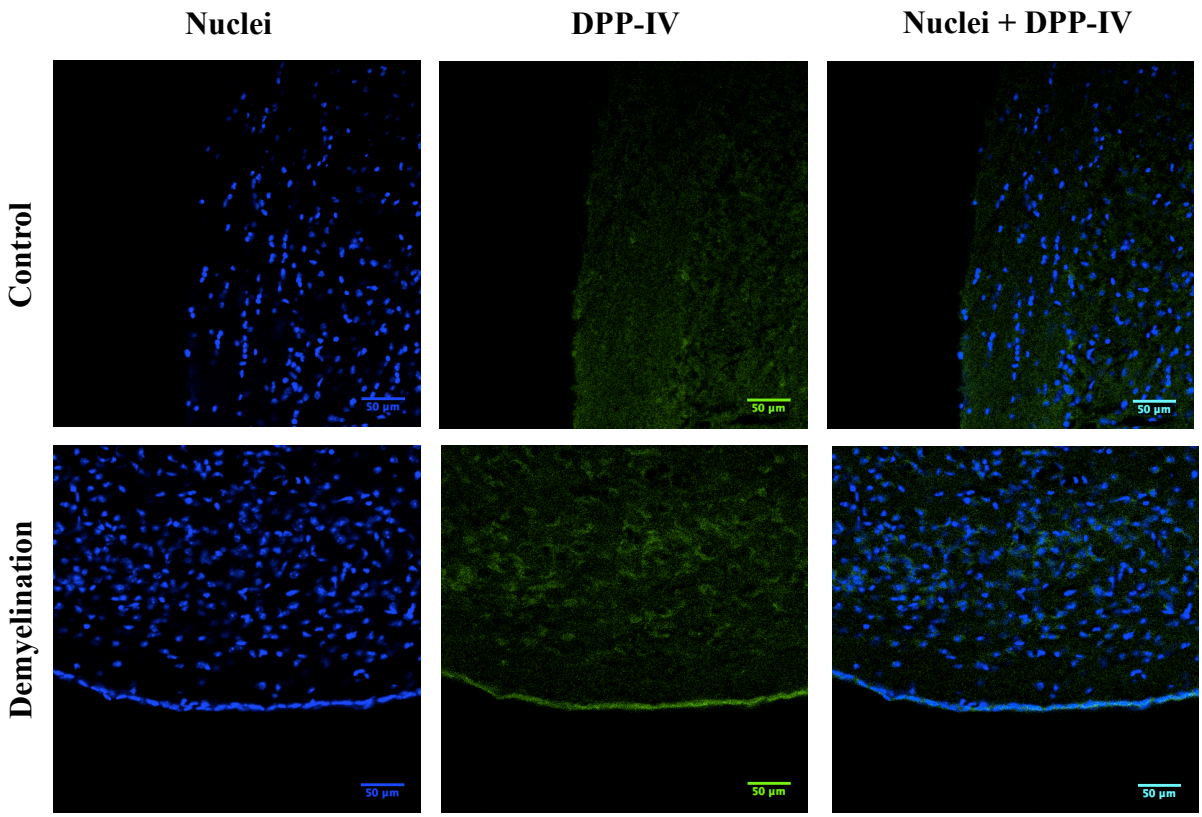

Figure 23. DPP-IV protein expression (immunostaining) in corpus callosum at peak of demyelination (W5) and early-remyelination (W7). Representative images of DPP-IV (green) corpus callosum localization, in control and demyelination phase (after 5 weeks of 0.2% CPZ intoxication). Nuclei are stained with DAPI (blue). Scale bar: 50 µm; n=1–2 for each group

6.2.6 GLP-1 expression

In the cerebellum, no differences in GLP-1 mRNA expression were observed between the groups, at week 5 and at week 7 (Figure 24).

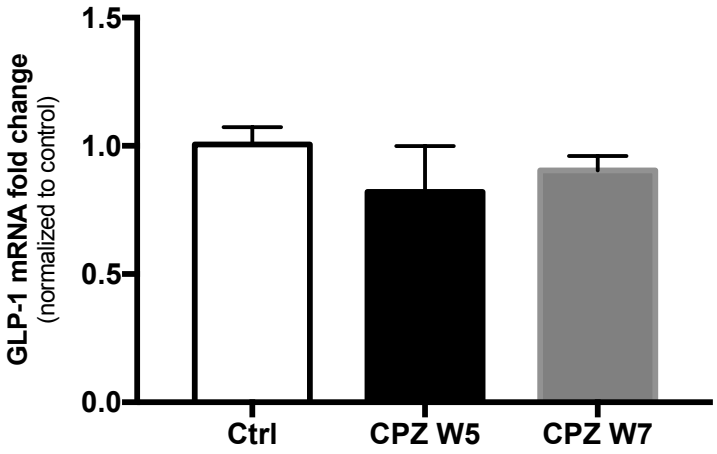

Figure 24. GLP-1 mRNA expression in the cerebellum at peak of demyelination (W5) and early-remyelination (W7). Quantification of GLP-1 gene expression in control (Ctrl), CPZ-intoxication (CPZ W5), and toxin withdrawal (CPZ W7) groups. Results were normalized to control and presented as means ± SEM. n=3 for Ctrl and n=4 for each CPZ group.

6.2.7 GLP-1R expression

CPZ intoxication induced no significant changes in GLP-1R mRNA expression in the cerebellum (Figure 25A). However, a significant decrease in GLP-1R protein content was observed after 5 weeks of exposition to the toxin (62.84 ± 8.62 % *vs* 100.00 ± 12.26 %, *p<0.05). After, 2 weeks of CPZ withdrawal (remyelination), GLP-1R protein levels approached the control ones (Figure 25B).

A

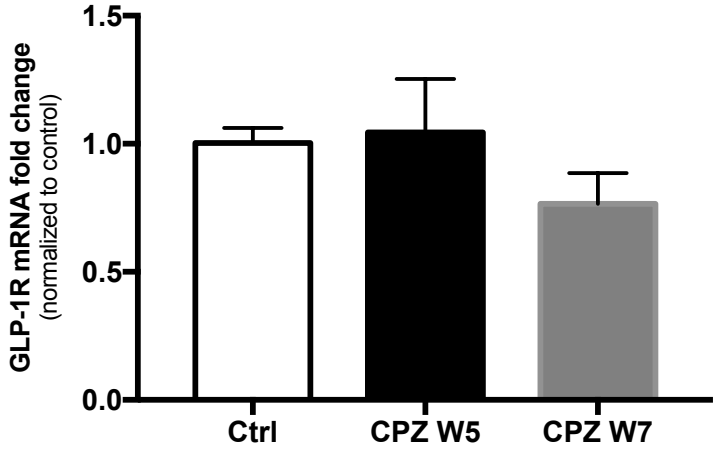

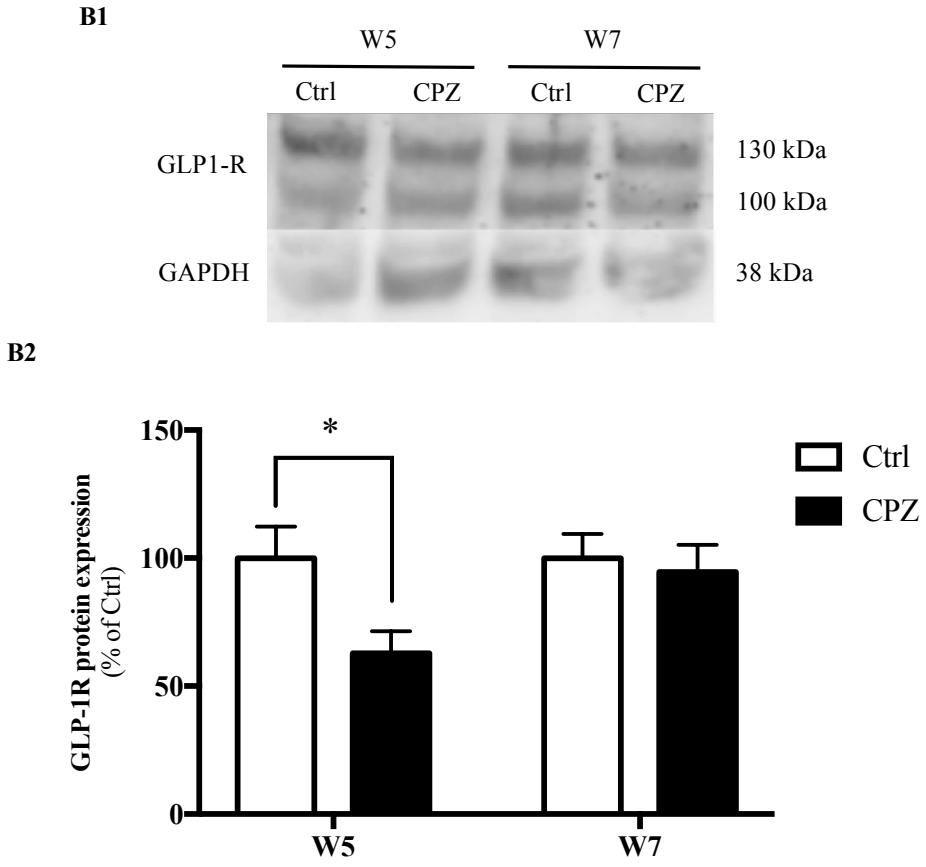

Figure 25. GLP-1R protein and gene expression in the cerebellum at peak of demyelination (W5) and early-remyelination (W7). (A) Quantification of GLP-1R gene expression in control (Ctrl), CPZ-intoxication (CPZ W5) and toxin withdrawal (CPZ W7) groups. Results were normalized to control and presented as means ± SEM. n=3 for Ctrl and n=4 for each CPZ group. (B1) Representative WB bands of GLP-1R expression in cerebellum. GAPDH was used as the internal control. (B2) Quantification of GFAP protein expression in cerebellum, after CPZ-intoxication (CPZ W5) and toxin withdrawal (CPZ W7) compared with a control for each group (Ctrl W5 and Ctrl W7). Results are expressed as percentage of the control and presented as means ± SEM; n=7 for each group; *p<0.05 vs Ctrl; t-test.

In the corpus callosum, a trend for increased GLP-1R expression (immunostaining) was observed in demyelinated samples, when compared with control. In the remyelination period, GLP-1R expression was reduced to a pattern similar to control (Figure 26).

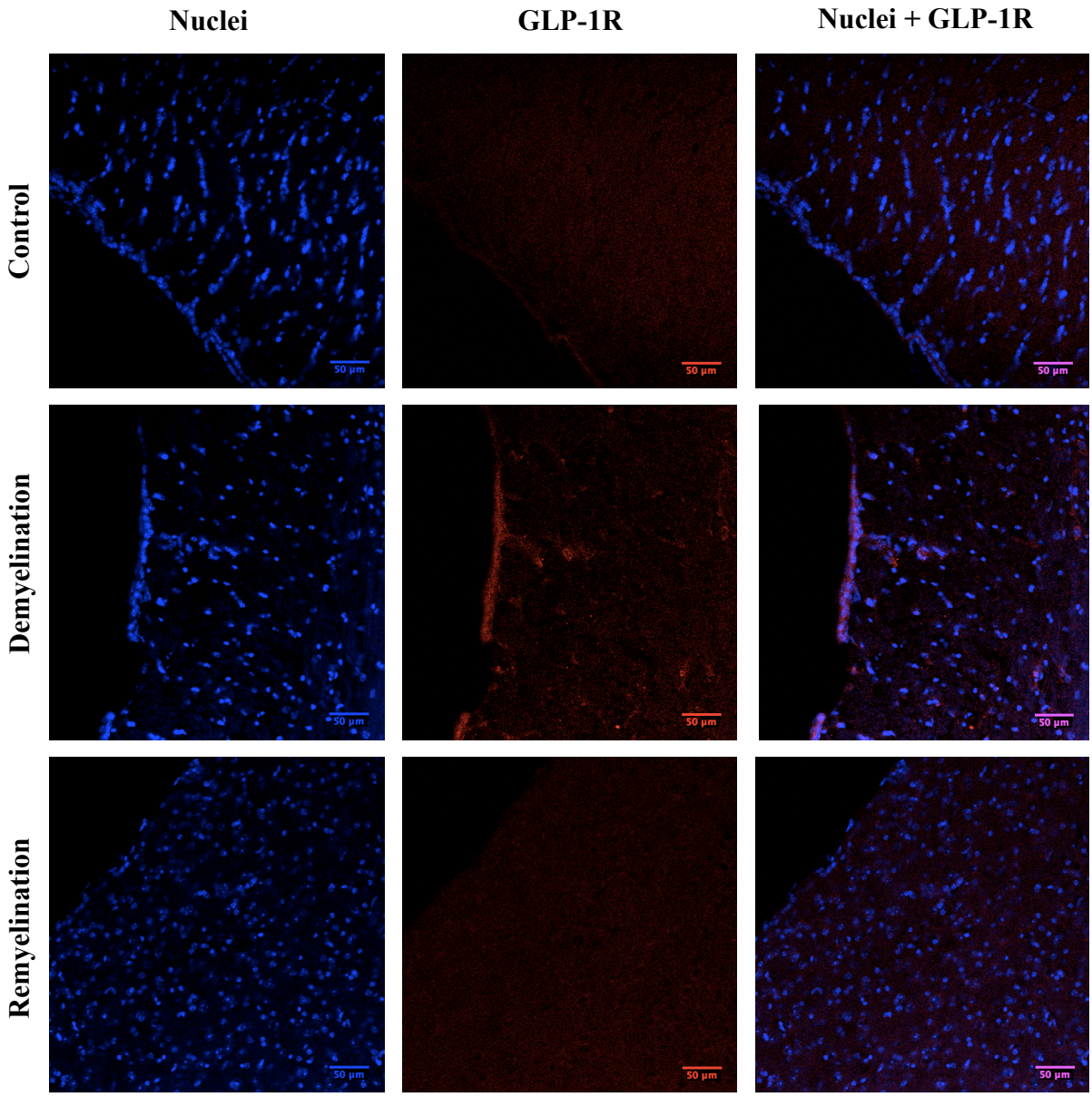

Figure 26. GLP-1R protein expression (immunostaining) in corpus callosum at peak of demyelination (W5) and early-remyelination (W7). Representative images of myelin-PLP (red) corpus callosum localization, in control, demyelination (after 5 weeks of 0.2% CPZ intoxication), and remyelination phases (after 2 weeks of CPZ-withdrawal). Nuclei are stained with DAPI (blue). Scale bar: 50 µm; n=1–2 for each group.

Chapter 7
Discussion

MS is an acquired, inflammatory demyelinating disease of the CNS, leading, subsequently, to the disruption of neuronal homeostasis (Compston & Coles, 2008; Dendrou *et al.*, 2015). The pathology of MS lesions is heterogeneous and several patterns suggesting predominant immune-mediated inflammation (pattern I and II) and primary oligodendrogliopathy (pattern III and IV) have been described (Lucchinetti *et al.*, 2000). Causative agent(s) of MS and a possible trigger of this disorder are still not well understood. The disease mainly begins in a person's late 20s to early 30s, runs a chronic and often debilitating course, and carries a large burden of suffering and expense for approximately 2.5 million people affected worldwide. MS is characterized by several symptoms such as fatigue, vision complications, numbness and tingling, muscle spasms and weakness, mobility problems, thinking and learning difficulties, depression and anxiety, although those can vary between patients (Compston & Coles, 2008; Dendrou *et al.*, 2015).

Currently available pharmacological options to manage MS (DMTs) only act by preventing disease's symptoms, not actually curing it, hence they are often associated with side effects. Furthermore, many forms of the disease, which are also the most severe, are still practically untreatable. Consequently, an efficient treatment for this disease is urgently needed. There is a vital need to deeply study and understand this neurological condition, so variable between patients. However, the human CNS is of difficult access, and can only be monitorized by non-invasive techniques or in a post-mortem examination. Therefore, the study of animal

models became crucial to better understand this disease and to search for more efficient and safe treatments.

The EAE is the animal model that better simulates the autoimmune features of this disease, although it lacks some key elements of the human disorder. Despite being the most commonly used model to study the autoimmune process of MS, it presents a great inflammatory background, which complicates the study of other important components of the pathophysiology. Toxic demyelination models are considered as the most suitable to study the processes involved in spontaneous demyelination and neural repair, mainly those not recruit a huge inflammatory burden.

Feeding C57BL/6 mice with the copper chelator CPZ induces reversible demyelination in relevant brain regions (considering MS pathophysiology) such as the corpus callosum and cerebellum. The CPZ-intoxication model correlates with newer histopathological data in MS and provides insights into the determinants of oligodendrocyte cell death, resembling pattern III lesions of MS (Lucchinetti *et al.*, 2000; Liebetanz & Merkler, 2006). More extensively, the model has been used to examine mechanisms of remyelination, obtained after CPZ withdrawal, with frequently surprising results. Although remyelination frequently occurs after demyelinating events, it is often incomplete. Therefore, this animal model of MS has increasingly attracted scientists to study the role of various molecular factors involved in de- and remyelination. Nevertheless, the behaviour impairment and several putative biochemical alterations related to CPZ-induced demyelination in the CNS remain to be elucidated. In fact, one of the major challenges in MS research is to better understand the remyelination failure in order to develop strategies able to efficiently restore myelin (Liebetanz & Merkler, 2006).

The main aim of this study was to characterize behaviour and biochemical alterations associated with demyelination and spontaneous remyelination in the CPZ animal model of MS. Therefore, C57BL/6 mice were studied at the peak of demyelination (after 5 weeks of CPZ administration, W5) and at an early-remyelination phase (after 2 weeks of CPZ withdrawal, W7).

First of all, concerning the behavioural alterations provoked by this compound we investigated, at those two different time points, the murine spontaneous exploration, short-term memory, anxiety-related behaviour and motor activity.

By applying the Y-maze test, a behavioural test for measuring the willingness of rodents to explore new environments, we wanted to see whether mice's short-term memory was, or not, affected by CPZ-intoxication. This test evaluates the spontaneous alternation behaviour (SAB), which is calculated as the ration between the number of alternations performed by the animal

and the total number of possible alternations. Rodents typically prefer to investigate a new arm of the maze rather than returning to one that was previously visited, so an animal with a lower SAB is an indicative of disturbed short-term memory. Obtained data showed no significant changes in mice's SAB, triggered by the toxin, during the peak of demyelination. Our results didn't resemble those observed by other studies, in which the intoxicated animals at the peak of demyelination showed a significantly lower SAB value, when compared with untreated controls; likewise, the memory loss is anticipated to be recovered after 2 weeks of remyelination period (Franco-Pons *et al.*, 2007; Makinodan *et al.*, 2009; Xu *et al.*, 2010, 2011; Skripuletz *et al.*, 2011).

Furthermore, experimental animals were studied in the open field test, in order to assess activity and behavioural response to a novel environment. Distance travelled in the central area, such as time spent in this zone, were evaluated as a measure of anxiety. In our study, no significant differences were observed between CPZ-treated and untreated (control) mice at both week 5 (demyelinated) and week 7 (remyelinated). However, there was a trend to a reduced number of rearings in demyelinated mice, compared with controls, with recover in remyelination period. Available scientific literature is controversial in what regards to the results of this test. Many groups affirm that mice treated with 0.2% CPZ are less anxious, and that white matter disorders induce an increased number of rearings, such as an increased activity in the centre of the open-field (Franco-Pons *et al.*, 2007; Wang *et al.*, 2013). Moreover, studies in humans have associated white matter disorders with impulsive behaviours (Silveri *et al.*, 2006). However, other studies, including the one by the enterprise Charles River, sustain the opposite, suggesting that demyelinated animals are more anxious, leading to less time spent in the central area, and decreased number of rearings, compared with controls (Makinodan *et al.*, 2009; Zainana *et al.*, 2015).

We also performed the splash test, in order to evaluate depression-related behaviour after intoxication with CPZ and further withdraw. Time spent in grooming is an indicative of animal's self-care and welfare. In the peak of demyelination (after 5 weeks of CPZ intoxication), the CPZ-treated mice showed a decrease in grooming, which is claimed to be a sign of depression and stress. Furthermore, this depressive behaviour disappeared after 2 weeks of detoxification, approaching controls. As far as we know, this is the first study that evaluated the splash test in this animal model of MS induced by CPZ intoxication. However this behaviour test has been used in other studies to evaluate signs of depression of mice under drugs' or antidepressant effects (Boulle *et al.*, 2014).

Apart from behaviour tests, we were interested in access possible biochemical changes in this CPZ model of MS. In this regard, expression of proteins (WB and IHC) and genes (RT-PCR) of interest in the cerebellum and corpus callosum was performed. We focused on the analysis (by WB and RT-PCR) of cerebellum samples, since it is one of the most affected areas of the CNS by this disease; in addition, it is a structure easily isolated in intact and well-defined conditions. On the other hand, corpus callosum is an area of difficult isolation, requiring careful removal of the surrounding structures, which complicates quantitative studies to be performed. To overcome these limitations and avoid possible misunderstand results, we decided to use corpus callosum only for protein expression by IHC, since it is easily identifiable, considering its proximity to the lateral ventricles of the brain.

Since MS is a demyelinating disease, it was crucial to analyse whether or not CPZ-intoxication was effective in destroying the axons' myelin cover. That effect was studied in cerebellum by quantifying protein and mRNA expression of myelin-PLP. This protein is one of the major myelin proteins from the CNS, playing an important role in the formation and maintenance of the multilamellar structure of the axons' cover. A trend to reduced protein expression (about 50%) in the cerebellum was found in the CPZ-treated mice *vs* control, at the peak of demyelination (week 5). Identical profile was encountered for mRNA expression in the same tissue at the same time-point. The values of protein and gene expression returned to control values after CPZ-withdrawal (remyelination). Furthermore, IHC analysis in the corpus callosum showed a significant decrease in PLP protein detection. These results are supported by previous ones, in which myelin-PLP and MBP mRNA expression, in corpus callosum, were strongly down-regulated already after 1 week of CPZ-intoxication, and reaching its lower levels (peak of demyelination) after 5 weeks (Gudi *et al.*, 2011; Steelman *et al.*, 2012). In addition, the same studies showed that after CPZ-withdrawal those values started normalizing; although PLP recovery was detected earlier than MBP, after 2 weeks of CPZ withdrawal myelin levels were partially restored (Gudi *et al.*, 2011; Steelman *et al.*, 2012).

Although neurodegeneration is the most prominent feature of MS, this disease is also accompanied by gliotic scar formation of chronic lesions. So, it is essential to study neurotoxicity markers, such as GFAP, the major intermediate astrocyte cytoskeletal protein. GFAP is a specific main constituent of intermediate filaments in astrocytes, which is released into the cerebrospinal fluid during pathological processes of the CNS. In MS, activation of astrocytes and microglia ultimately leads to astrogliosis which is reflected in an accumulation of GFAP in the MS lesions. As expected, we found an overexpression of protein GFAP levels in the cerebellum of CPZ-treated mice at the peak of demyelination (W5 CPZ), when compared

with healthy controls (W5 Ctrl), indicating that degenerative processes with astrogliosis are increased in MS, such as expected in human patients. Those values were significantly normalized after 2 weeks of CPZ withdrawal (W7 CPZ), when compared with W5 CPZ. Previous studies analysed astrogliosis by GFAP immunostaining, indicating that few GFAP positive astrocytes were seen in the corpus callosum in untreated controls, contrasting with a remarkable astrogliosis after 3 weeks of exposition to the toxin. Additionally, mice undergoing remyelination had less GFAP intensity than those treated for 5 weeks, in agreement with our results (Gudi *et al.*, 2011; Steelman *et al.*, 2012).

In MS, the immune-neuronal interaction involves the responsiveness of neurons and glia to inflammatory cytokines released by infiltrating lymphocytes and activated microglia, such as TNF-α and IL-1β (Arnett *et al.*, 2001; Serra-de-Oliveira *et al.*, 2015). In this study we analysed the expression of those cytokines in the CPZ model of demyelination and remyelination. Results showed a significantly increased expression of both cytokines in the cerebellum in the peak of demyelination, when compared with healthy subjects. In addition, those values were normalized in an early demyelination phase. These cytokines are mostly described in the EAE model of MS and in the human disease; however they have also been described in the CPZ model, by other works, which validate our results. Those results showed other similarities between this toxic model and the human disease (Arnett *et al.*, 2001; Serra-de-Oliveira *et al.*, 2015).

One of the main focus of this work was to analyse whether the DPP-IV/GLP-1 pathway is impaired in this animal model of MS. This pathway, responsible for maintaining physiological glucose homeostasis, is best known for its involvement in T2DM pathophysiology. A disruption in this pathway (increased DPP-IV levels and activity, followed by significantly decreased GLP-1 contents) leads to hyperglycemia and insulin resistance. Growing evidences suggest that dysfunction of this pathway, somehow, may increase the risk for neurodegeneration/neuronal death, and functional and structural brain changes, culminating in cognitive dysfunction that underlies some dementia-type disorders, such as AD, PD and possibly MS (Luchsinger *et al.*, 2004; Harkavyi & Whitton, 2010; Hölscher, 2012, 2014; Duarte *et al.*, 2013).

Our results showed no differences in DPP-IV protein and mRNA expression in the cerebellum between the CPZ-exposed and control groups. However, IHC images showed the presence and possibly an increased expression of the enzyme in the affected areas, indicating the possibility of using of DPP-IV as a pharmacological target. Furthermore, measurement of

the enzyme activity is still needed, once this could be more active at the peak of demyelination (Steinbrecher *et al.*, 2001).

Focusing in one of the main DPP-IV, GLP-1 mRNA expression was not affected in this animal model. However, GLP-1R protein expression was significantly decreased after 5 weeks of CPZ-intoxication, in cerebellum samples. Furthermore, those values were restored to normal ones in the second week of remyelination, suggesting an involvement in the processes of demyelination and remyelination. Our results, yet preliminary, do not invalidate our hypothesis previously postulated.

GLP-1 mRNA is being normally expressed in the intoxicated animal, but that does not necessary mean that protein levels were maintained unchanged. Since DPP-IV enzyme activity might be higher in the peak of demyelination, this can result in a significant decrease in GLP-1 protein expression. Further studies are mandatory to confirm, or deny, this possibility. Likewise, the diminished expression of the GLP-1 might provoke a downregulation in its receptor expression, since it is not being needed. Furthermore, GLP-1R expression, in the hypothalamus, has also been studied in T2DM patients indicating a decrease due to the deregulation of feeding behaviour and glucose homeostasis (Ten Kulve *et al.*, 2016). Additionally, a study in the EAE model demonstrated a modulation effect of DPP-IV in $CD4^+$ T lymphocytes. This group was able to partially supress EAE symptoms by administration of a DPP-IV inhibitor in vivo. Likewise, clinical signs reduction was associated with reduced CNS inflammation (TNF-α) (Steinbrecher *et al.*, 2001).

Overall, our results, combined with previous ones from other groups, maintain opened, and intact, the possibility of DPP-IV contribution to the development and/or maintenance of the disease, such as a possible pharmacological target. Further studies are needed to complement our new findings.

Chapter 8
Conclusions

The main conclusions of our study focused on the characterization of an animal model of MS induced by CPZ intoxication are:

The experimental approach based on CPZ intoxication during 5 weeks and further detoxication by CPZ withdrawal during the following 2 weeks was able to create the expected conditions of demyelination (at week 5) and early remyelination (at week 7).

In fact, this model presents at the peak of demyelination (week 5) the anticipated reduced expression of myelin-PLP protein levels in the corpus callosum (IHC data), accompanied by diminished protein and gene myelin-PLP in the cerebellum (WB and RT-PCR). Coherently, the reduced expression of both protein and gene was abolished after the period of early remyelination (week 7). This is extremely relevant in validating all the concepts beyond the model.

Furthermore, our experimental conditions and time-points were also able to mimic the gliosis component of the disease, revealed by the significantly increased GFAP protein expression in both the cerebellum (WB) and corpus callosum (IHC) at the peak of demyelination (week 5). This effect was remarkable reduced, or even abolished, after CPZ withdrawal during the following 2 weeks (early remyelination stage).

This profile of neurotoxicity was accompanied by a depression-related behaviour (splash test) and by a trend to changes on parameters of anxiety (open field test), without changes on short-term memory (Y-maze test).

The pathological process of demyelination was accompanied by an overexpression of IL-1β and TNF-α in the cerebellum, followed by normalization in the remyelination induced by CPZ withdrawal, suggesting the existence of an inflammatory component of CNS injury, also in this model.

Although yet inconclusive, the changes observed on the expression of DPP-IV, GLP-1 and GLP-1R in the cerebellum and corpus callosum maintain opened the possibility to use this pathway as an interesting and relevant therapeutic target in MS. Further studies are mandatory to complement our preliminary data.

Lastly, the existence of relevant changes on several important parameters of the disease in the cerebellum opens good perspectives to use this brain structure/region as a relevant complementary sample to study the pathophysiological molecular mechanisms underlying MS development, as well as to search for novel therapeutic targets and drugs.

REFERENCES

Acs, P. & Kalman, B. (2012) Pathogenesis of multiple sclerosis: what can we learn from the cuprizone model. In Springer (ed), *Autoimmunity: Methods and Protocols, Methods in Molecular Biology, Vol. 900*. New York, pp. 403–431.

Aharoni, R. (2010) Immunomodulatory drug treatment in multiple sclerosis. *Expert Rev. Neurother.*, **10**, 1423–1436.

Arnett, H. a, Mason, J., Marino, M., Suzuki, K., Matsushima, G.K., & Ting, J.P. (2001) TNF alpha promotes proliferation of oligodendrocyte progenitors and remyelination. *Nat. Neurosci.*, **4**, 1116–1122.

Aviles-Olmos, I., Limousin, P., Lees, A., & Foltynie, T. (2013) Parkinson's disease, insulin resistance and novel agents of neuroprotection. *Brain*, **136**, 374–384.

Belbasis, L., Bellou, V., Evangelou, E., Ioannidis, J.P.A., & Tzoulaki, I. (2015) Environmental risk factors and multiple sclerosis: an umbrella review of systematic reviews and meta-analyses. *Lancet Neurol.*, **14**, 263–273.

Benetti, F., Ventura, M., Salmini, B., Ceola, S., Carbonera, D., Mammi, S., Zitolo, A., D'Angelo, P., Urso, E., Maffia, M., Salvato, B., & Spisni, E. (2010) Cuprizone neurotoxicity, copper deficiency and neurodegeneration. *Neurotoxicology*, **31**, 509–517.

Biton, A., Bank, U., Täger, M., Ansorge, S., Reinhold, D., Lendeckel, U., & Brocke, S. (2006) Dipeptidyl peptidase IV (DP IV, CD26) and aminopeptidase N (APN, CD13) as regulators of T cell function and targets of immunotherapy in CNS inflammation. *Int. Immunopharmacol.*, **6**, 1935–1942.

Boulle, F., Massart, R., Stragier, E., Païzanis, E., Zaidan, L., Marday, S., Gabriel, C., Mocaer, E., Mongeau, R., & Lanfumey, L. (2014) Hippocampal and behavioral dysfunctions in a mouse model of environmental stress: normalization by agomelatine. *Transl. Psychiatry*, **4**, e485.

Buchwalow, I.B. & Böcker, W. (2010) *Immunohistochemistry: Basics and Methods*. Springer Berlin Heidelberg, Berlin, Heidelberg.

Campbell, J.E. & Drucker, D.J. (2013) Pharmacology, physiology, and mechanisms of incretin hormone action. *Cell Metab.*, **17**, 819–837.

Chari, D.M. (2007) Remyelination in multiple sclerosis. *Int. Rev. Neurobiol.*, **79**, 589–620.

Chou, J.C.T., Lin, C.-Y., & Long, H. (2011) Glucagon-like peptide-1 receptor (GLP-1R) agonists for treating autoimmune disorders, WO 2011/024110 A2.

Cohen, J.A. & Rae-Grant, A. (2010) *Handbook of Multiple Sclerosis*, 1st edn. Springer Healthcare, London.

Compston, A. & Coles, A. (2008) Multiple sclerosis. *Lancet*, **372**, 1502–1517.

Compston, A., Confavreux, C., Lassmann, H., McDonald, I., Miller, D., Noseworthy, J., Smith, K., & Wekerle, H. (2006) *McAlpine's Multiple Sclerosis*, 4th edn. Churchil Livingstone Elsevier, Philadelphia.

Dendrou, C.A., Fugger, L., & Friese, M.A. (2015) Immunopathology of multiple sclerosis. *Nat. Rev. Immunol.*, **15**, 545–558.

Denic, a, Johnson, A., & Bieber, A. (2011) The relevance of animal models in multiple sclerosis research. *Pathophysiology*, **18**, 1–16.

Drucker, D.J. (2006) The biology of incretin hormones. *Cell Metab.*, **3**, 153–165.

Duarte, A.I., Candeias, E., Correia, S.C., Santos, R.X., Carvalho, C., Cardoso, S., Plácido, A., Santos, M.S., Oliveira, C.R., & Moreira, P.I. (2013) Crosstalk between diabetes and brain: Glucagon-like peptide-1 mimetics as a promising therapy against neurodegeneration. *Biochim. Biophys. Acta - Mol. Basis Dis.*, **1832**, 527–541.

Ezcurra, M., Reimann, F., Gribble, F.M., & Emery, E. (2013) Molecular mechanisms of incretin hormone secretion. *Curr. Opin. Pharmacol.*, **13**, 922–927.

Fenu, G., Lorefice, L., Frau, F., Coghe, G.C., Marrosu, M.G., & Cocco, E. (2015) Induction and escalation therapies in multiple sclerosis. *Antiinflamm. Antiallergy. Agents Med. Chem.*, **14**, 26–34.

Fischer, M.T., Wimmer, I., Hoftberger, R., Gerlach, S., Haider, L., Zrzavy, T., Hametner, S., Mahad, D., Binder, C.J., Krumbholz, M., Bauer, J., Bradl, M., & Lassmann, H. (2013) Disease-specific molecular events in cortical multiple sclerosis lesions. *Brain*, **136**, 1799–1815.

Franco-Pons, N., Torrente, M., Colomina, M.T., & Vilella, E. (2007) Behavioral deficits in the cuprizone-induced murine model of demyelination/remyelination. *Toxicol. Lett.*, **169**, 205–213.

Frischer, J.M., Weigand, S.D., Guo, Y., Kale, N., Parisi, J.E., Pirko, I., Mandrekar, J., Bramow, S., Metz, I., Brück, W., Lassmann, H., & Lucchinetti, C.F. (2015) Clinical and pathological insights into the dynamic nature of the white matter multiple sclerosis plaque. *Ann. Neurol.*, **78**, 710–721.

Grigoriadis, N. & van Pesch, V. (2015) A basic overview of multiple sclerosis immunopathology. *Eur. J. Neurol.*, **22**, 3–13.

Gudi, V., Škuljec, J., Yildiz, Ö., Frichert, K., Skripuletz, T., Moharregh-Khiabani, D., Voß, E., Wissel, K., Wolter, S., & Stangel, M. (2011) Spatial and temporal profiles of growth factor expression during CNS demyelination reveal the dynamics of repair priming. *PLoS One*, **6**, e22623.

Haan, M. (2006) Therapy Insight: type 2 diabetes mellitus and the risk of late-onset Alzheimer's disease. *Nat Clin Pr. Neurol*, **2**, 159–166.

Harkavyi, A. & Whitton, P.S. (2010) Glucagon-like peptide 1 receptor stimulation as a means of neuroprotection. *Br. J. Pharmacol.*, **159**, 495–501.

Harlow, D.E., Honce, J.M., & Miravalle, A.A. (2015) Remyelination therapy in multiple Sclerosis. *Front. Neurol.*, **6**, 1–13.

Hauser, S.L. & Oksenberg, J.R. (2006) The neurobiology of multiple sclerosis: genes, inflammation, and neurodegeneration. *Neuron*, **52**, 61–76.

Hemmer, B., Nessler, S., Zhou, D., Kieseier, B., & Hartung, H.-P. (2006) Immunopathogenesis and immunotherapy of multiple sclerosis. *Nat. Clin. Pract. Neurol.*, **2**, 201–211.

Hölscher, C. (2012) Potential role of glucagon-like peptide-1 (GLP-1) in neuroprotection. *CNS Drugs*, **26**, 871–882.

Hölscher, C. (2014) Central effects of GLP-1: New opportunities for treatments of neurodegenerative diseases. *J. Endocrinol.*, **221**, T31–T41.

Iwanowski, P. & Losy, J. (2015) Immunological differences between classical phenothypes of multiple sclerosis. *J. Neurol. Sci.*, **349**, 10–14.

Kazafeos, K. (2011) Incretin effect: GLP-1, GIP, DPP4. *Diabetes Res. Clin. Pract.*, **93S**, S32–

S36.

Keough, M.B., Rogers, J.A., Zhang, P., Jensen, S.K., Stephenson, E.L., Chen, T., Hurlbert, M.G., Lau, L.W., Rawji, K.S., Plemel, J.R., Koch, M., Ling, C.-C., & Yong, V.W. (2016) An inhibitor of chondroitin sulfate proteoglycan synthesis promotes central nervous system remyelination. *Nat Commun*, **7**, 1–12.

Kim, S.C., Schneeweiss, S., Glynn, R.J., Doherty, M., Goldfine, A.B., & Solomon, D.H. (2014) Dipeptidyl peptidase-4 inhibitors in type 2 diabetes may reduce the risk of autoimmune diseases: a population-based cohort study. *Ann. Rheum. Dis.*, **0**, 1–9.

Kipp, M., Clarner, T., Dang, J., Copray, S., & Beyer, C. (2009) The cuprizone animal model: new insights into an old story. *Acta Neuropathol.*, **118**, 723–736.

Kurien, B.T. & Scofield, R.H. (2015) *Western Blotting*, Methods in Molecular Biology. Springer New York, New York, NY.

Lambeir, A.-M., Durinx, C., Scharpé, S., & De Meester, I. (2003) Dipeptidyl-peptidase IV from bench to bedside: an update on structural properties, functions, and clinical aspects of the enzyme DPP IV. *Crit. Rev. Clin. Lab. Sci.*, **40**, 209–294.

Liebetanz, D. & Merkler, D. (2006) Effects of commissural de- and remyelination on motor skill behaviour in the cuprizone mouse model of multiple sclerosis. *Exp. Neurol.*, **202**, 217–224.

Lijun, C., Li, D., Feng, P., Li, L., Xue, G.-F., Ji, C., Li, G., & Hölscher, C. (2016) A novel dual GLP-1 and GIP receptor agonist is neuroprotective in the MPTP mouse model of Parkinson's disease by increasing expression of BNDF. *Brain Res.*, **11**, 326–331.

Lin, F. & Prichard, J. (2015) *Handbook of Practical Immunohistochemistry*. Springer New York, New York, NY.

Llufriu, S., Blanco, Y., Martinez-Heras, E., Casanova-Molla, J., Gabilondo, I., Sepulveda, M., Falcon, C., Berenguer, J., Bargallo, N., Villoslada, P., Graus, F., Valls-Sole, J., & Saiz, A. (2012) Influence of corpus callosum damage on cognition and physical disability in multiple sclerosis: a multimodal study. *PLoS One*, **7**, 1–7.

Lucchinetti, C., Brück, W., Parisi, J., Scheithauer, B., Rodriguez, M., & Lassmann, H. (2000) Heterogeneity of multiple sclerosis lesions: Implications for the pathogenesis of demyelination. *Ann. Neurol.*, **47**, 707–717.

Luchsinger, J., Tang, M.-X., Shea, S., & Mayeux, R. (2004) Hyperinsulinemia and risk of Alzheimer disease. *Neurology*, **63**, 1187–1192.

Machado, A., Valente, F., Reis, M., Saraiva, P., & Silva, R. (2010) Esclerose Múltipla – Implicações Sócio-Económicas. *Acta Med. Port.*, **23**, 631–640.

Makinodan, M., Yamauchi, T., Tatsumi, K., Okuda, H., Takeda, T., Kiuchi, K., Sadamatsu, M., Wanaka, A., & Kishimoto, T. (2009) Demyelination in the juvenile period, but not in adulthood, leads to long-lasting cognitive impairment and deficient social interaction in mice. *Prog. Neuro-Psychopharmacology Biol. Psychiatry*, **33**, 978–985.

Marinelli, C., Bertalot, T., Zusso, M., Skaper, S.D., & Giusti, P. (2016) Systematic review of pharmacological properties of the oligodendrocyte lineage. *Front. Cell. Neurosci.*, **10**, 1–19.

Michel, L., Larochelle, C., & Prat, A. (2015) Update on treatments in multiple sclerosis. *Presse Med.*, **44**, e137–e151.

Mix, E., Meyer-Rienecker, H., Hartung, H.P., & Zettl, U.K. (2010) Animal models of multiple sclerosis-potentials and limitations. *Prog. Neurobiol.*, **92**, 386–404.

Nylander, A. & Hafler, D. a (2012) Multiple sclerosis. *J Clin Invest*, **122**, 1180–1188.

Palavra, F., Reis, F., & Almeida, L. (2014) Remyelination in multiple sclerosis – how close are we? *J Neurol Neurophysiol*, **5**, 1–6.

Paz Soldán, M.M., Novotna, M., Abou Zeid, N., Kale, N., Tutuncu, M., Crusan, D.J., Atkinson, E.J., Siva, A., Keegan, B.M., Pirko, I., Pittock, S.J., Lucchinetti, C.F., Weinshenker, B.G., Rodriguez, M., & Kantarci, O.H. (2015) Relapses and disability accumulation in progressive multiple sclerosis. *Neurology*, **84**, 81–88.

Polman, C.H., Reingold, S.C., Banwell, B., Clanet, M., Cohen, J.A., Filippi, M., Fujihara, K., Havrdova, E., Hutchinson, M., Kappos, L., Lublin, F.D., Montalban, X., O'Connor, P., Sandberg-Wollheim, M., Thompson, A.J., Waubant, E., Weinshenker, B., & Wolinsky, J.S. (2011) Diagnostic criteria for multiple sclerosis: 2010 Revisions to the McDonald criteria. *Ann. Neurol.*, **69**, 292–302.

Popescu, B.F.G. & Lucchinetti, C.F. (2012) Pathology of demyelinating diseases. *Annu. Rev. Pathol. Mech. Dis.*, **7**, 185–217.

Popescu, B.F.G., Pirko, I., & Lucchinetti, C.F. (2013) Pathology of multiple sclerosis: where

do we stand? *Contin. Lifelong Learn. Neurol.*, **19**, 901–921.

Procaccini, C., De Rosa, V., Pucino, V., Formisano, L., & Matarese, G. (2015) Animal models of multiple sclerosis. *Eur. J. Pharmacol.*, **759**, 182–191.

Ransohoff, R.M. (2012) Animal models of multiple sclerosis: the good, the bad and the bottom line. *Nat. Neurosci.*, **15**, 1074–1077.

Ransohoff, R.M., Hafler, D. a., & Lucchinetti, C.F. (2015) Multiple sclerosis—a quiet revolution. *Nat. Rev. Neurol.*, **11**, 134–142.

Rasmussen, H.B., Branner, S., Wiberg, F.C., & Wagtmann, N. (2003) Crystal structure of human dipeptidyl peptidase IV/CD26 in complex with a substrate analog. *Nat. Struct. Biol.*, **10**, 19–25.

Röhrborn, D., Wronkowitz, N., & Eckel, J. (2015) DPP4 in diabetes. *Front. Immunol.*, **6**, 1–20.

Seino, Y., Fukushima, M., & Yabe, D. (2010) GIP and GLP-1, the two incretin hormones: Similarities and differences. *J. Diabetes Investig.*, **1**, 8–23.

Seino, Y. & Yabe, D. (2013) Glucose-dependent insulinotropic polypeptide and glucagon-like peptide-1: Incretin actions beyond the pancreas. *J. Diabetes Investig.*, **4**, 108–130.

Serra-de-Oliveira, N., Boilesen, S.N., Prado de França Carvalho, C., LeSueur-Maluf, L., Zollner, R. de L., Spadari, R.C., Medalha, C.C., & Monteiro de Castro, G. (2015) Behavioural changes observed in demyelination model shares similarities with white matter abnormalities in humans. *Behav. Brain Res.*, **287**, 265–275.

Silveri, M.M., Rohan, M.L., Pimentel, P.J., Gruber, S.A., Rosso, I.M., & Yurgelun-Todd, D.A. (2006) Sex differences in the relationship between white matter microstructure and impulsivity in adolescents. *Magn. Reson. Imaging*, **24**, 833–841.

Simmons, S.B., Pierson, E.R., Lee, S.Y., & Goverman, J.M. (2013) Modeling the heterogeneity of multiple sclerosis in animals. *Trends Immunol.*, **34**, 410–422.

Skripuletz, T., Gudi, V., Hackstette, D., & Stangel, M. (2011) De- and remyelination in the CNS white and grey matter induced by cuprizone: The old, the new, and the unexpected. *Histol. Histopathol.*, **26**, 1585–1597.

Star, B.J. Van der, Vogel, D., Kipp, M., & Amor; Sandra (2012) In Vitro and In Vivo Models of Multiple Sclerosis. *CNS Neurol. Disord. - Drug Targets*, **11**, 570–588.

Steelman, A.J., Thompson, J.P., & Li, J. (2012) Demyelination and remyelination in anatomically distinct regions of the corpus callosum following cuprizone intoxication. *Neurosci. Res.*, **72**, 32–42.

Steinbrecher, a, Reinhold, D., Quigley, L., Gado, A., Tresser, N., Izikson, L., Born, I., Faust, J., Neubert, K., Martin, R., Ansorge, S., & Brocke, S. (2001) Targeting dipeptidyl peptidase IV (CD26) suppresses autoimmune encephalomyelitis and up-regulates TGF-beta 1 secretion in vivo. *J. Immunol.*, **166**, 2041–2048.

Ten Kulve, J.S., van Bloemendaal, L., Balesar, R., RG, I.J., Swaab, D.F., Diamant, M., la Fleur, S.E., & Alkemade, A. (2016) Decreased hypothalamic glucagon-like peptide-1 receptor expression in type 2 diabetes patients. *J Clin Endocrinol Metab*, **101**, 2122–2129.

Torkildsen, Ø., Brunborg, L.A., Myhr, K.-M., & Bø, L. (2008) The cuprizone model for demyelination. *Acta Neurol. Scand.*, **117**, 72–76.

Tornes, L., Conway, B., & Sheremata, W. (2014) Multiple sclerosis and the cerebellum. *Neurol. Clin.*, **32**, 957–977.

Wahlsten, D. (2011) Chapter 3: Tests of Mouse Behavior. In *Mouse Behavioral Testing – How to Use Mice in Behavioral Neuroscience*, 1 st. edn. Academic Press, London, pp. 39–51.

Wang, H., Li, C., Wang, H., Mei, F., Liu, Z., Shen, H.Y., & Xiao, L. (2013) Cuprizone-induced demyelination in mice: age-related vulnerability and exploratory behavior deficit. *Neurosci. Bull.*, **29**, 251–259.

Wingerchuk, D.M. & Carter, J.L. (2014) Multiple sclerosis: current and emerging disease-modifying therapies and treatment strategies. *Mayo Clin. Proc.*, **89**, 225–240.

Xu, H., Yang, H.-J., McConomy, B., Browning, R., & Li, X.-M. (2010) Behavioral and neurobiological changes in C57BL/6 mouse exposed to cuprizone: effects of antipsychotics. *Front. Behav. Neurosci.*, **4**, 1–10.

Xu, H., Yang, H.-J., Rose, G.M., & Li, X.-M. (2011) Recovery of behavioral changes and compromised white matter in C57BL/6 mice exposed to cuprizone: effects of antipsychotic drugs. *Front. Behav. Neurosci.*, **5**, 31.

Yadav, S.K., Mindur, J.E., Ito, K., & Dhib-Jalbut, S. (2015) Advances in the immunopathogenesis of multiple sclerosis. *Curr. Opin. Neurol.*, **28**, 206–219.

Yazbeck, R., Howarth, G.S., & Abbott, C.A. (2009) Dipeptidyl peptidase inhibitors, an

emerging drug class for inflammatory disease? *Trends Pharmacol. Sci.*, **30**, 600–607.

Zainana, A., Puoliväli, J., Heikkinen, T., Hodgson, R., & Nurmi, A. (2015) Behavioral characterization of the cuprizone model of demyelination in mice. *Charles River*, **223**.